

## CHAPTER 2

# NONLINEARITIES AND SATURATION

*Stephan Fauve, Raymond Hide,  
David Hughes, Irene Moroz,  
François Pétrélis.*

In this chapter, we focus on the effects of nonlinearity. After general considerations in Section 2.1, we investigate the *rôle* of nonlinearity in saturating the growth of the magnetic field for a dynamo with a spatially periodic flow in Section 2.2. We then turn to the more general situation of saturation in the vicinity of the dynamo threshold; first in the low  $Re$  limit in Section 2.3 and then in the high  $Re$  limit in Section 2.4. We then address the issue of dynamo saturation in flows strongly affected by rotation (with planetary applications in mind) in Section 2.5, and we present some conjectures for the magnetic field generated by a turbulent flow when  $Re$  and  $Rm$  are both large in Section 2.6. Mean field dynamo saturation (with astrophysical applications in mind) is discussed in Section 2.7. Finally, we return in Section 2.8 to the apparently simple disk dynamo model used as an introductory example in Chapter 1 to show how rich the nonlinear dynamical behaviour can be.

### 2.1. GENERAL CONSIDERATIONS

The study of dynamo action is motivated both by laboratory experiments and by observations of astrophysical or geophysical magnetic fields. Recently, the first homogeneous fluid dynamos have been successfully demonstrated: in Karlsruhe (Stieglitz & Müller, 2001) using a flow in an array of pipes set-up in order to mimic a spatially periodic flow proposed by G.O. Roberts (1972), and in Riga (Gailitis *et al.*,

2001) using a Ponomarenko-type flow (Ponomarenko, 1973). Although there were no doubts about self-generation of magnetic fields by Roberts or Ponomarenko-type laminar flows, these experiments have displayed several interesting features:

- The observed thresholds are in rather good agreement with theoretical predictions (Busse *et al.*, 1996; Rädler *et al.*, 1998; Gailitis *et al.*, 2002) made by considering only the laminar mean flow and neglecting the small-scale turbulent fluctuations that are present in both experiments.
- The nature of the dynamo bifurcation, stationary for the Karlsruhe experiment or oscillatory (Hopf) in the Riga experiment, is also in agreement with laminar models.
- On the contrary, the saturation level of the magnetic field, due to the Lorentz force back reaction on the flow, cannot be predicted with a laminar flow model. It has been shown indeed that different scaling laws exist in the supercritical dynamo regime depending on the magnitude of the Reynolds number (Pétrélis & Fauve, 2001).

These observations raise several questions: we do not discuss here the effect of turbulence on the dynamo threshold (Fauve & Pétrélis, 2003) or the characteristics of magnetic field fluctuations (Bourgoin *et al.*, 2002) but rather try to understand the scaling law for the mean magnetic field amplitude above the dynamo threshold. To wit, we take into account the back reaction of the magnetic field on the velocity field. We thus try to solve the dynamic dynamo problem, or in other words, to find a nonlinear equation for the amplitude of the linearly unstable mode at the bifurcation. Solving this equation determines the sub-critical or super-critical nature of the bifurcation and in the later case, the amplitude of the magnetic field as a function of the distance to the dynamo threshold.

Both the Karlsruhe and Riga experiments operate in the vicinity of dynamo threshold (typically 10% above threshold) and it is unlikely that a laboratory experiment could reach high  $R_m$  values (say 10 times critical) because the power needed to drive a turbulent flow increases like the cubic power of its mean velocity. It is also possible that the Geodynamo does not operate too far from threshold but it is not the case of other astrophysical objects for which huge values of  $R_m$  can be reached. Weakly nonlinear theory is of little use in these situations as well as in the case of a strongly subcritical bifurcation that may be the case of the Geodynamo.

Magnetic fields exist on a wide range of scales in astrophysics. Their orders of magnitude as well as some associated relevant parameters for planets, stars and our galaxy are given in Table I. It is perhaps meaningless to try to compare these data because these astrophysical objects have strongly different physical properties. However, we may observe that the strength of the magnetic field  $\mathbf{B}$  is not strongly related

**Table I** - Approximate parameters and magnetic field strength of some astrophysical objects (Zeldovich *et al.*, 1983). The size  $L$  is based on the typical length (radius for spheres, thickness for disks) of the conducting region (not of the full object). The magnetic field strength is an averaged one (in the case of the Sun, the field can locally be  $10^3$  times stronger). The resistivity  $\eta$  is usually based on molecular estimates, except in the Galaxy for which it represents “ambipolar diffusion”.

	the Galaxy	Sun	Jupiter	Earth core	White dwarfs	Neutron stars
$ \mathbf{B} $ (T)	$10^{-10}$	$10^{-4}$	$4 \times 10^{-4}$	$10^{-4}$	$10^2 - 10^4$	$10^6 - 10^9$
$\rho$ ( $\text{kg m}^{-3}$ )	$10^{-21}$	1	$10^3$	$10^4$	$10^5 - 10^{12}$	$10^{13} - 10^{18}$
$L$ (m)	$10^{19}$	$2 \times 10^8$	$5 \times 10^7$	$3 \times 10^6$	$10^6$	$10^4 - 10^6$
$\eta$ ( $\text{m}^2 \text{s}^{-1}$ )	$10^{17}$	$10^3$	10	2		
$ \mathbf{B} ^2 L^3 / 2\mu_0$	$10^{43}$	$4 \times 10^{22}$	$10^{22}$	$2 \times 10^{17}$		
$ \mathbf{B} ^2 L \eta / 2\mu_0$	$10^{22}$	$10^9$	$4 \times 10^7$	$2 \times 10^5$		

to the size of the object  $L$ , but seems to increase with its density  $\rho$ . If instead of looking at the intensity of the magnetic field, we consider the typical magnetic energy of the object  $\langle |\mathbf{B}|^2 \rangle L^3 / 2\mu_0$  ( $\mu_0$  is the magnetic permeability of vacuum), we find the expected ordering from the galaxy to the Earth. We may also consider the typical value of the Joule dissipation. To wit, we divide the magnetic energy by the characteristic magnetic diffusion time  $L^2/\eta$  (let us recall that  $\eta = (\mu_0\sigma)^{-1}$ , where  $\sigma$  is the electrical conductivity of the medium). We thus get an idea of the minimum amount of power which is necessary to maintain the magnetic field against Joule dissipation. Again, we observe the expected ordering from the galaxy to the Earth. Note that these values have certainly been underestimated. First, they are estimated from the visible (poloidal) part of the magnetic field, and are thus strongly underestimated if the azimuthal field inside the body is large compared to the poloidal component. Second, we have assumed that the length scale of the gradients of the magnetic field is the size  $L$  of the conducting medium. Magnetic energy at smaller scales will lead to a shorter diffusion time scale and thus to a higher dissipated power.

Let us first recall the induction equation (1.14) and the Navier-Stokes equation (1.26) that we restrict to incompressible flows ( $\nabla \cdot \mathbf{u} = 0$ ), without the Coriolis force but with the Lorentz force (1.17) included

$$\frac{\partial \mathbf{B}}{\partial t} = \nabla \times (\mathbf{u} \times \mathbf{B}) + \eta \Delta \mathbf{B}, \quad (2.1a)$$

$$\partial_t \mathbf{u} + (\mathbf{u} \cdot \nabla) \mathbf{u} = -\nabla \left( \frac{p}{\rho} + \frac{|\mathbf{B}|^2}{2\mu_0} \right) + \nu \Delta \mathbf{u} + \frac{1}{\mu_0 \rho} (\mathbf{B} \cdot \nabla) \mathbf{B}. \quad (2.1b)$$

The flow is created, either by moving solid boundaries or by a body force added to the Navier-Stokes equation. We have to develop equations (2.1a,b) close to the dynamo threshold in order to derive an amplitude equation for the growing magnetic field. If the dynamo bifurcation is found to be supercritical, this allows us to calculate the saturated magnetic field.

Thus, even in the simplest configuration, the problem involves three dimensionless parameters. One may choose, the Reynolds number,  $Re$ , the magnetic Reynolds number,  $Rm$ , and the Lundquist number,  $\langle |\mathbf{B}|^2 \rangle \mu_0 (\sigma L)^2 / \rho$ , leading in general to the following form of law

$$\frac{\langle |\mathbf{B}|^2 \rangle \mu_0 (\sigma L)^2}{\rho} = f(Rm, Re). \quad (2.2)$$

Another possible choice is obtained by replacing  $Re$  by the magnetic Prandtl number,  $Pm = Rm/Re = \mu_0 \sigma \nu$ . For most fluids,  $Pm \ll 1$  i.e.  $Re \gg Rm$ .

In general, the analytic determination of  $f$  using weakly nonlinear perturbation theory in the vicinity of the dynamo threshold is tractable only in the unrealistic case  $Pm \gg 1$  such that the dynamo bifurcates from a laminar flow ( $Re \ll 1$ ). For  $Pm \ll 1$ , many hydrodynamic bifurcations occur first and the flow becomes turbulent before the dynamo threshold.

We first present the structure of the perturbation analysis of weakly nonlinear theory in the vicinity of the dynamo threshold in the tractable case  $Re \ll 1$ . We then discuss the realistic situation ( $Re \gg 1$ ) and, using dimensional or phenomenological arguments, show that the expression of the generated magnetic field as a function of the fluid parameters strongly differs from the case  $Re \ll 1$ .

Astrophysical or geophysical dynamos involve many more parameters due to the nature of the driving of the flow. A particularly important one is the global rotation rate. We shortly review how this may affect the saturation of the magnetic field. Finally, we discuss some conjectures in the limit of  $Re$  and  $Rm$  both large for a turbulent flow without global rotation.

## 2.2. SATURATION OF A DYNAMO GENERATED BY A PERIODIC FLOW

It has been shown by G.O. Roberts (1970, 1972) that many spatially periodic flows generate a magnetic field at a large scale compared to their spatial periodicity. In that case the weakly nonlinear problem above the bifurcation threshold is also more easily tractable (Gilbert & Sulem, 1990). We recall some of these linear and nonlinear results obtained for periodic flows and that have been recently used to discuss

the results of the Karlsruhe experiment (Tilgner & Busse, 2001; Rädler *et al.*, 2002).

### 2.2.1. SCALE SEPARATION

We consider a spatially periodic velocity field with wavelength  $\ell$  and zero mean value, and we assume that a magnetic field  $\mathbf{B}_0$  is generated on a spatial scale  $L$ . A magnetic field with spatial periodicity  $\ell$  is generated by the interaction of  $\mathbf{B}_0$  with the flow. We thus write

$$\mathbf{B} = \mathbf{B}_0 + \mathbf{b}, \quad (2.3)$$

with  $\langle \mathbf{b} \rangle = 0$ , where  $\langle \cdot \rangle$  stands for the spatial average over one wavelength  $\ell$ . Inserting (2.3) in the induction equation, and averaging over space, we get the evolution equation for the mean field  $\mathbf{B}_0$

$$\partial_t \mathbf{B}_0 = \nabla \times \langle \mathbf{u} \times \mathbf{B} \rangle + \eta \Delta \mathbf{B}_0. \quad (2.4)$$

Subtracting (2.4) from the induction equation, we get the evolution equation for the fluctuating field  $\mathbf{b}$

$$\partial_t \mathbf{b} = \nabla \times (\mathbf{u} \times \mathbf{B}_0 + \mathbf{u} \times \mathbf{b} - \langle \mathbf{u} \times \mathbf{b} \rangle) + \eta \Delta \mathbf{b}. \quad (2.5)$$

We have to find  $\mathbf{b}$  as a function of  $\mathbf{B}_0$  using equation (2.5) in order to get a closed equation for the mean field from (2.4). Equation (2.5) may be solved easily if  $b = |\mathbf{b}|$  is small compared to  $B_0 = |\mathbf{B}_0|$ ; we then have at leading order a diffusion equation for  $\mathbf{b}$  with a source term depending on  $\mathbf{B}_0$  and the velocity field. Then, we get

$$\eta \frac{b}{\ell^2} \sim \frac{u B_0}{\ell}, \quad \text{thus} \quad b \sim \frac{u \ell}{\eta} B_0. \quad (2.6)$$

Using this expression for  $b$  in order to estimate  $\langle \mathbf{u} \times \mathbf{b} \rangle$ , which does not depend any more on  $\ell$  after being averaged, we get from (2.4) the following condition for dynamo onset on  $u_c = |\mathbf{u}|$ :

$$\frac{u_c^2 \ell}{\eta} \frac{B_0}{L} \sim \frac{\eta B_0}{L^2}, \quad \text{thus} \quad u_c \sim \frac{\eta}{\sqrt{L \ell}}. \quad (2.7)$$

We first observe that  $b \sim \sqrt{\ell/L} B_0 \ll B_0$  provided that  $\ell \ll L$ . In this limit, the magnetic Reynolds number defined on each eddy of size  $\ell$  is thus very small whereas the one defined on  $L$  is large. We observe that the relevant definition here for the magnetic Reynolds number would be

$$\text{Rm}_2 \equiv \frac{|\mathbf{u}| \sqrt{L \ell}}{\eta}, \quad (2.8)$$

the critical value of which for dynamo onset is of order one. Consequently, even if the above mechanism works, we cannot reach the dynamo onset just by increasing scale separation. For  $\eta$  and  $|\mathbf{u}|$  fixed, it does not help to decrease  $\ell$ . Scale separation makes it possible to keep the magnetic Reynolds number small at dynamo onset if it is defined on the scale of each eddy,  $\ell$ . In this limit, the field  $\mathbf{B}_0$  is not strongly distorted by the fluid motion. This allows easier analytical calculations.

### 2.2.2. THE G.O. ROBERTS DYNAMO

We consider the spatially periodic flow (see Section 1.4.1) with velocity field

$$\mathbf{u}(x, y, z) = (U \sin ky, U \cos kx, V(\sin kx + \cos ky)) . \quad (2.9)$$

We have  $\langle \mathbf{u} \rangle = 0$  and the mean helicity is  $h = \langle \mathbf{u} \cdot \nabla \times \mathbf{u} \rangle = -2kUV$ . Assuming that  $b$  is small compared to  $B_0 = |\mathbf{B}_0|$ , we get from equation (2.5)

$$\mathbf{b} \approx \frac{1}{\eta k} (U B_2 \cos ky, -U B_1 \sin kx, V B_1 \cos kx - V B_2 \sin ky) , \quad (2.10)$$

where  $\mathbf{B}_0 = (B_1, B_2, B_3)$ . We thus get

$$\langle \mathbf{u} \times \mathbf{b} \rangle \approx \frac{UV}{\eta k} \begin{pmatrix} 1 & 0 & 0 \\ 0 & 1 & 0 \\ 0 & 0 & 0 \end{pmatrix} \mathbf{B}_0 . \quad (2.11)$$

We observe that if a large scale field exists along the  $x$  or  $y$ -axis, the cooperative effect of small scale periodic fluctuations is to drive a current parallel to the large scale field. This has been understood by Parker (1955) and is due to the helical nature of the flow. Any field  $B_1$  along the  $x$ -axis is distorted in the vertical  $(x, z)$ -plane by the  $z$ -component of the flow of amplitude  $V$ . The field is twisted out of the  $(x, z)$ -plane by the toroidal component of the flow of amplitude  $U$ . This drives field loops in the  $(y, z)$ -plane, i.e. a current parallel to  $x$ , which generates a magnetic field with a non-zero component along the  $y$ -axis,  $B_2$ .  $B_2$  can then regenerate  $B_1$  through the same process. The mean electromotive force  $\langle \mathbf{u} \times \mathbf{b} \rangle$  in the mean field equation (2.4) was described by Steenbeck & Krause (1966) as the “ $\alpha$ -effect” (see for instance Krause & Rädler, 1980). In this terminology, G.O. Roberts’ dynamo is an  $\alpha^2$ -dynamo. Defining  $\alpha = UV/\eta k$ , we have for a mean field of the form  $\mathbf{B}_0(z, t) = (B_1, B_2, 0)$ , where  $B_1$  and  $B_2$  satisfy

$$\frac{\partial B_1}{\partial t} = -\alpha \frac{\partial B_2}{\partial z} + \eta \frac{\partial^2 B_1}{\partial z^2} , \quad \frac{\partial B_2}{\partial t} = \alpha \frac{\partial B_1}{\partial z} + \eta \frac{\partial^2 B_2}{\partial z^2} . \quad (2.12a,b)$$

Defining  $A = B_1 + iB_2$ , we get

$$\frac{\partial A}{\partial t} = -i\alpha \frac{\partial A}{\partial z} + \eta \frac{\partial^2 A}{\partial z^2} . \quad (2.13)$$

The linear stability analysis of the solution  $A = 0$  (i.e.  $\mathbf{B}_0 = 0$ ) is straightforward. We consider normal modes of the form  $A \propto \exp(\eta t \pm iKz)$  and get from (2.13) the dispersion relation

$$\eta = \pm|\alpha K| - \eta K^2, \quad (2.14)$$

which shows that there exists a branch of unstable modes at long enough wavelength ( $K < |\alpha|/\eta$ ).

We observe that dynamo action vanishes if  $U \rightarrow 0$  or  $V \rightarrow 0$  in agreement with anti-dynamo theorems. It is interesting to consider the behavior of  $\alpha$  when the magnetic Reynolds number becomes larger. To wit, the calculation of  $\mathbf{b}$  should be performed at higher orders in equation (2.5). Solving perturbatively this equation for  $\mathbf{b}$  as an expansion in powers of  $U/\eta k$ , one gets

$$\alpha = \frac{UV}{\eta k} \left( 1 - \frac{U^2}{2\eta^2 k^2} + \dots \right). \quad (2.15)$$

$\alpha$  increases linearly with  $V$  but its behavior as a function of  $U$  is more complex. It first increases but reaches a maximum and then decreases as  $U$  is increased. This behavior is due to the expulsion of the transverse field by the rotating eddies, as already shown in Rädler *et al.* (1998) by numerically solving (2.5). It has been found that  $\alpha$  decreases toward zero at large Rm. Note however that the large Rm limit should be considered carefully. As stated above, the great simplification of scale separation results from the fact that the magnetic Reynolds number evaluated on the small scale of the flow is small whereas the one evaluated on the large scale of the mean field is large. This is clearly apparent in our second order result (2.15). Truncating the expansion in  $|\mathbf{u}|/\eta k$  is not accurate if Rm is too large such that the magnetic Reynolds number related to the azimuthal motion of the eddies becomes of order 1.

The  $\alpha$ -effect has been demonstrated experimentally by directly measuring the mean electromotive force generated by a helical flow of liquid sodium in the presence of an external magnetic field (Steenbeck *et al.*, 1968). Self-generation of a magnetic field by the  $\alpha$ -effect has been achieved recently, using a periodic arrangement of counter-rotating and counter-current helical vortices that mimic G.O. Roberts' flow. Axial and azimuthal sodium flows are driven by pumps in an array of helical ducts immersed in a cylinder (Karlsruhe experiment, Stieglitz & Müller, 2001).

### 2.2.3. SATURATION OF DYNAMOS DRIVEN BY THE $\alpha$ -EFFECT

Saturation of an  $\alpha$ -dynamo may involve the generation of a large scale flow generated by the large scale magnetic field (Malkus & Proctor, 1975). If this large scale flow is not forbidden by the geometrical configuration, it is likely to exist without a

magnetic field and to play a *rôle* already at the level of the kinematic dynamo problem. On the contrary, if any large scale flow is forbidden, as in the Karlsruhe experiment, the saturation is due to the modification of the small scale velocity field which reduces the electromotive force related to the  $\alpha$ -effect. In that case, the perturbation method based on scale separation can be easily extended to the study of the dynamic dynamo problem, as shown in the case of the G.O. Roberts' flow (Gilbert & Sulem, 1990). The mean field equation (2.4) is unchanged but the mean electromotive force  $\langle \mathbf{u} \times \mathbf{b} \rangle$  should be calculated using both equation (2.5) and the Navier-Stokes equation (2.1b). The simplest way to generate G.O. Roberts' flow is to add a body force  $\mathbf{f} = -\nu \Delta \mathbf{u}^0$  to (2.1b) where  $\mathbf{u}^0$  is given by (2.9). In the presence of a magnetic field, we have to leading order

$$\eta \Delta \mathbf{b} \approx -(\mathbf{B}_0 \cdot \nabla) \mathbf{u}, \quad \nu \Delta \mathbf{u} + \frac{(\mathbf{B}_0 \cdot \nabla) \mathbf{b}}{\rho \mu_0} + \mathbf{f} \approx \mathbf{0}. \quad (2.16a,b)$$

The first equation is formally unchanged compared to the kinematic calculation although  $\mathbf{u}$  is no longer prescribed, but should be obtained by solving the linear system (2.16a,b). The velocity field  $\mathbf{u}^0$  in the absence of magnetic field is modified by the Lorentz force. Note that  $(\mathbf{B} \cdot \nabla) \mathbf{B} \approx (\mathbf{B}_0 \cdot \nabla) \mathbf{b}$  up to terms of order  $\sqrt{\ell/L} \ll 1$  from the assumption of scale separation. Solving (2.16a,b), we get for the electromotive force

$$\langle \mathbf{u} \times \mathbf{b} \rangle \approx \frac{UV}{\eta k} \begin{pmatrix} \left(1 + \frac{\sigma B_1^2}{\rho \nu k^2}\right)^{-1} & 0 & 0 \\ 0 & \left(1 + \frac{\sigma B_2^2}{\rho \nu k^2}\right)^{-1} & 0 \\ 0 & 0 & 0 \end{pmatrix} \mathbf{B}_0. \quad (2.17)$$

We thus find that the  $\alpha$ -effect saturates when the magnetic field amplitude increases because of the action of the Lorentz force on the velocity field. This saturation should not be confused with that observed for large  $|\mathbf{u}|$  in (2.15) which is a linear effect due to flux expulsion. Defining

$$\tilde{B}_i^2 = \frac{\sigma B_i^2}{\rho \nu k^2}, \quad (2.18)$$

we obtain from the mean field equation (2.4)

$$\frac{\partial \tilde{B}_1}{\partial t} = -\alpha \frac{\partial}{\partial z} \left[ \frac{\tilde{B}_2}{(1 + \tilde{B}_2^2)^2} \right] + \eta \frac{\partial^2 \tilde{B}_1}{\partial z^2}, \quad (2.19a)$$

$$\frac{\partial \tilde{B}_2}{\partial t} = -\alpha \frac{\partial}{\partial z} \left[ \frac{\tilde{B}_1}{(1 + \tilde{B}_1^2)^2} \right] + \eta \frac{\partial^2 \tilde{B}_2}{\partial z^2}. \quad (2.19b)$$

Numerical simulation of these equations shows that the magnetic field cascades to large spatial scales during the saturation process (Gilbert & Sulem, 1990).

We thus observe that the saturated mean magnetic field obeys the following scaling law

$$\langle B_0^2 \rangle \propto \frac{\rho\nu}{\sigma\ell^2} (\text{Rm} - \text{Rm}_c), \quad (2.20)$$

with  $\text{Rm} = \sqrt{UV}\sqrt{Ll}/\eta$ .

In the case of an isotropic flow, a nonlinear evolution equation for the mean field can be easily obtained by symmetry considerations. We get

$$\partial_T \mathbf{B}_0 = \alpha \nabla \times (1 - \gamma \mathbf{B}_0^2) \mathbf{B}_0 + \eta \Delta \mathbf{B}_0. \quad (2.21)$$

In the absence of large scale flow, we expect similar nonlinearities in the case of  $\alpha^2$ -dynamos generated by small scale turbulent fluctuations. Phenomenological descriptions leading to equations of the form (2.21) have been proposed (Kraichnan, 1979; Meneguzzi *et al.*, 1981, Gruzinov & Diamond, 1994). We do not expect however that  $\gamma$  corresponds to the laminar scaling when the Reynolds number of the flow is large (see below). Different scaling laws have been also proposed in relation to the helicity injection rate and dynamics.

## 2.3. SATURATION IN THE LOW Re LIMIT IN THE VICINITY OF THE DYNAMO THRESHOLD

### 2.3.1. A PONOMARENKO TYPE DYNAMO AS A TRACTABLE PROBLEM WITHOUT SCALE SEPARATION

In the absence of scale separation, it is much more difficult to derive an amplitude equation for the magnetic field in the vicinity of the bifurcation threshold. We have performed such a calculation using the following trick. We slightly modified Ponomarenko's original configuration (a cylinder in solid body rotation and translation along its axis, embedded in an infinite static medium of the same conductivity with which it is in perfect electrical contact) by considering that the rotating cylinder is hollow and filled with a liquid metal of the same conductivity. This gives a very simple flow, i.e. solid body rotation and translation, which is the simplest way to avoid turbulence at dynamo onset. The kinematic dynamo problem is thus the same as that studied by Ponomarenko. However, above the dynamo threshold, the flow is modified by the Lorentz force and is expected to saturate the growth of the magnetic field.

We will not present here the calculation of the amplitude equation (see Nuñez *et al.*, 2001) but simply show the structure of the perturbation analysis.

### 2.3.2. STRUCTURE OF THE PERTURBATION ANALYSIS

The structure of the weakly nonlinear analysis above threshold is as follows: the forcing generates a velocity field  $\mathbf{u}_f$  and the dynamo bifurcates for  $\mathbf{u}_f = \mathbf{u}_c$ , i.e.  $\text{Rm} = \text{Rm}_c$ . We write (2.1a) in the form

$$\mathcal{L}(\mathbf{B}^{(0)}) = 0, \quad (2.22)$$

where  $\mathbf{B}^{(0)}$  is the neutral mode at threshold and  $\mathcal{L}$  is a linear operator that depends on the bifurcation structure (stationary or Hopf bifurcation). In the case of the Ponomarenko dynamo, we have a Hopf bifurcation with neutral modes of the form (Ponomarenko, 1973)

$$\mathbf{B}^{(0)} = A(T)\mathbf{B}_p + c.c. = A(T)\mathbf{b}_p(r) \exp i(m\theta + kz + \omega_0 t) + c.c., \quad (2.23)$$

where  $(r, \theta, z)$  are cylindrical coordinates and c.c. stands for the complex conjugate of the previous expression.

The flow is forced slightly above threshold,  $\mathbf{u}_f = \mathbf{u}_c + \varepsilon\mathbf{u}_d + \dots$ , with  $\varepsilon = (\text{Rm} - \text{Rm}_c)/\text{Rm}_c \ll 1$ . In addition, the leading order flow distortion by the Lorentz force,  $\varepsilon\mathbf{u}^{(1)}$ , yields

$$\mathbf{u} = \mathbf{u}_f + \varepsilon\mathbf{u}^{(1)} + \dots. \quad (2.24)$$

We have for  $\mathbf{B}$  
$$\mathbf{B} = \sqrt{\varepsilon}(\mathbf{B}^{(0)} + \varepsilon\mathbf{B}^{(1)} + \dots). \quad (2.25)$$

We first compute  $\mathbf{u}^{(1)}$  from equation (2.1b) at order  $\varepsilon$ ,

$$\begin{aligned} \partial_t \mathbf{u}^{(1)} + (\mathbf{u}_c \cdot \nabla) \mathbf{u}^{(1)} + (\mathbf{u}^{(1)} \cdot \nabla) \mathbf{u}_c = & -\frac{1}{\rho} \nabla \left( p_1 + \frac{|\mathbf{B}^{(0)}|^2}{2\mu_0} \right) \\ & + \nu \Delta \mathbf{u}^{(1)} + \frac{1}{\mu_0 \rho} (\mathbf{B}^{(0)} \cdot \nabla) \mathbf{B}^{(0)}. \end{aligned} \quad (2.26)$$

If  $\text{Pm} \gg 1$ , the flow is laminar at the dynamo threshold, and the Lorentz force is mostly balanced by the modification of the viscous force, thus

$$|\mathbf{u}^{(1)}| \propto \frac{|\mathbf{B}^{(0)}|^2 L}{\mu_0 \rho \nu}. \quad (2.27)$$

We get from equation (2.1a) at order  $\varepsilon$ ,

$$\mathcal{L}(\mathbf{B}^{(1)}) = \partial_T \mathbf{B}^{(0)} - \nabla \times (\mathbf{u}_d \times \mathbf{B}^{(0)}) - \nabla \times (\mathbf{u}^{(1)} \times \mathbf{B}^{(0)}), \quad (2.28)$$

where  $T = \varepsilon t$  is the slow time scale of  $\mathbf{B}^{(0)}$  slightly above threshold. The amplitude equation for  $\mathbf{B}^{(0)}$  that governs the saturation of the magnetic field is obtained by applying the solvability condition to (2.28),

$$\langle \mathbf{C} | \mathcal{L}(\mathbf{B}^{(0)}) \rangle = \langle \mathbf{C} | \partial_T \mathbf{B}^{(0)} \rangle - \langle \mathbf{C} | \nabla \times (\mathbf{u}_d \times \mathbf{B}^{(0)}) \rangle - \langle \mathbf{C} | \nabla \times (\mathbf{u}^{(1)} \times \mathbf{B}^{(0)}) \rangle = 0, \quad (2.29)$$

where  $\langle \mathbf{a} | \mathbf{b} \rangle = \int \mathbf{a} \cdot \mathbf{b} \, d\mathbf{x}$ . Thus

$$\langle \mathbf{C} | \partial_T \mathbf{B}^{(0)} \rangle = \langle \mathbf{C} | \nabla \times (\mathbf{u}_d \times \mathbf{B}^{(0)}) \rangle + \langle \mathbf{C} | \nabla \times (\mathbf{u}^{(1)} \times \mathbf{B}^{(0)}) \rangle, \quad (2.30)$$

where  $\mathbf{C}$  is an eigenvector of the adjoint problem. The first term on the right hand side of (2.30) corresponds to the linear growth rate of the magnetic field whereas the second describes the nonlinear saturation due to the modified velocity field  $\mathbf{u}^{(1)}$ . For nonlinearly saturated solutions, we thus get  $u_d \propto u^{(1)}$ . In the vicinity of threshold,  $\mu_0 \sigma L(u_f - u_c) \propto \text{Rm} - \text{Rm}_c$ , and we obtain

$$\langle |\mathbf{B}|^2 \rangle \propto \frac{\rho\nu}{\sigma L^2} (\text{Rm} - \text{Rm}_c). \quad (2.31)$$

### 2.3.3. THE LAMINAR SCALING

We call (2.31) the ‘‘laminar scaling’’, obtained for  $\text{Re} \ll 1$  and characterized by the fact that  $B \rightarrow 0$  if  $\nu \rightarrow 0$  with all the other parameters fixed.

For a Ponomarenko type flow, we obtained a supercritical bifurcation (Nuñez *et al.*, 2001). The leading order nonlinear effects tend to saturate the growing magnetic field because the Lorentz force slows down the motion and hence diminishes the induction. We obtained for the magnetic field at saturation  $\mathbf{B}_{sat}$ ,

$$\mathbf{B}_{sat} = 2.82 \sqrt{\frac{\rho\nu}{\sigma R^2}} \sqrt{\text{Rm} - \text{Rm}_c} \text{Re} \{ \mathbf{B}_p \}, \quad (2.32)$$

where  $\mathbf{B}_p$  is the neutral mode of the Ponomarenko dynamo.

The magnetic energy has the form of equation (2.31), what we called the laminar scaling because the Lorentz force is balanced by the perturbation in velocity through a viscous term. Close to onset, there is obviously no equipartition of energy because the magnetic energy tends to zero with  $\text{Rm} - \text{Rm}_c$  while the kinetic energy is finite. There is neither any simple balance between viscous dissipation and Joule dissipation. For Joule dissipation we have  $P_j \propto \int |\mathbf{j}|^2 dV \propto \int |\nabla \times \mathbf{B}|^2 dV \propto (\text{Rm} - \text{Rm}_c)$ . Concerning viscous dissipation  $P_\nu$ , it is proportional to the square of the stress tensor. This tensor is linear in the total velocity and is thus proportional to  $\mathbf{u}^{(1)}$  because the stress tensor of  $\mathbf{u}_f$  is zero (solid body rotation and translation). Hence  $P_\nu \propto |\mathbf{u}^{(1)}|^2 \propto (\text{Rm} - \text{Rm}_c)^2$ . In this particular case, with no viscous dissipation

at onset, we observe that most of the input power is dissipated by Joule effect close to the dynamo onset. In more complex laminar flows, Joule dissipation is of course negligible compared to viscous dissipation just above the dynamo threshold.

More realistic helical flow geometries have been considered (Bassom & Gilbert, 1997) but the saturating magnetic field has been computed only in the limit  $Re \gg Rm \gg 1$  for which it is difficult to have controlled approximations. However, the result also shares the main property of the laminar scaling,  $B \rightarrow 0$  if  $\nu \rightarrow 0$  with all the other parameters fixed.

## 2.4. SATURATION IN THE HIGH $Re$ LIMIT IN THE VICINITY OF THE DYNAMO THRESHOLD

### 2.4.1. DIMENSIONAL ARGUMENTS

We show now that we can take advantage of the characteristics of experimental dynamos to find the correct scaling of the magnetic field above the dynamo threshold (Pétréris & Fauve, 2001). We have already mentioned that  $P_m \ll 1$  for most fluids. More precisely,  $P_m < 10^{-5}$  for all liquid metals. Thus, the Reynolds number is larger than several millions at the dynamo threshold ( $Rm_c$  is in the range 10 – 100). In addition, the power needed to generate this turbulent flow increases like the cubic power of the driving velocity. Consequently, most experimental dynamos should:

- (i) bifurcate from a strongly turbulent flow regime,
- (ii) operate in the vicinity of their bifurcation threshold.

Although (i) makes almost impossible any realistic analytical calculation or direct numerical simulation, the above two characteristics allow an estimation of the non-linearly saturated magnetic field above  $Rm_c$  using dimensional analysis. Our goal is thus to find the expression of  $f$  in equation (2.2) in the limits (i)  $Re \rightarrow \infty$  and (ii)  $Rm - Rm_c \rightarrow 0$ : (i) implies that the momentum is mostly transported by turbulent fluctuations. Consequently, using the basic assumption of fully developed turbulence, we can neglect the kinematic viscosity, thus  $Re$ . (ii) implies that the dependence of  $\langle B^2 \rangle$  on  $Rm$  is proportional to  $Rm - Rm_c$ , as expected for a supercritical bifurcation close to threshold. In other words,  $U = |\mathbf{u}|$  is no longer a free parameter, but should take approximately the value corresponding to the dynamo threshold. Thus, (i) and (ii) reduce the number of parameters from 6 to 4, and the saturated value of the magnetic field can be obtained using dimensional analysis, to

give

$$\langle |\mathbf{B}|^2 \rangle \propto \frac{\rho}{\mu_0(\sigma L)^2} (\text{Rm} - \text{Rm}_c). \quad (2.33)$$

There is no paradox in the fact that the saturated magnetic field is inversely proportional to the square of the electric conductivity and to the square of the typical lengthscale of the flow. This does not mean that one should have  $\sigma$  and  $L$  small in order to observe large values of  $|\mathbf{B}|$  since  $\text{Rm} = \text{Rm}_c$  will be then achieved for a larger flow velocity. Using the typical velocity  $U_c = |\mathbf{u}|$  at dynamo threshold, we can write (2.33) in the form,  $\langle |\mathbf{B}|^2 \rangle / \mu_0 \rho U_c^2 \propto (\text{Rm} - \text{Rm}_c) / \text{Rm}_c^2$ , which shows that the system is very far from equipartition of energy in the vicinity of the dynamo threshold. We emphasize also that the interaction parameter,  $N = \sigma L \langle |\mathbf{B}|^2 \rangle / \rho |\mathbf{u}|$ , is much smaller than one. It is such that

$$N \propto \text{Rm} - \text{Rm}_c. \quad (2.34)$$

#### 2.4.2. HIGH Re DYNAMOS CLOSE TO THE BIFURCATION THRESHOLD

For  $\text{Pm} \ll 1$  or  $\text{Re} \gg 1$ , we can recover the “turbulent scaling” (2.33) using the structure of the perturbation analysis presented for laminar dynamos. The only difference is that if  $\text{Re} \gg 1$ , we have to balance the Lorentz force with the inertial instead of the viscous terms in (2.26). We thus get  $|\mathbf{B}_{\text{laminar}}| \propto |\mathbf{B}_{\text{turbulent}}| \text{Pm}^{1/2}$ ; consequently the two scalings strongly differ for experiments using liquid metals ( $\text{Pm} < 10^{-5}$ ).

It may be instructive to replace  $\nu$  by the turbulent viscosity,  $\nu_T \propto |\mathbf{u}| L$ , in the laminar scaling (2.31). Using  $|\mathbf{u}| \approx \text{Rm}_c / \mu_0 \sigma L$ , we have

$$\langle |\mathbf{B}|^2 \rangle \propto \frac{\rho \nu_T}{\sigma L^2} (\text{Rm} - \text{Rm}_c) \propto \frac{\rho}{\mu_0(\sigma L)^2} (\text{Rm} - \text{Rm}_c). \quad (2.35)$$

We thus recover the turbulent scaling. However, dimensional arguments of the previous section do not require any assumption about the turbulent viscosity expression and are thus clearer.

The Karlsruhe (Stieglitz & Müller, 2001) and Riga (Gailitis *et al.*, 2001) experiments have recently reported values of the saturated mean magnetic field of order 10 mT, roughly 10% above threshold. Both experiments used liquid sodium ( $\mu_0 \sigma \approx 10 \text{ m}^{-2} \text{ s}$ ,  $\rho \approx 10^3 \text{ kg m}^{-3}$ ). The inner diameter of the Riga experiment is  $L = 0.25 \text{ m}$ . The spatial periodicity of the flow used in the Karlsruhe experiment is of the same order of magnitude, within a cylinder of radius 0.85 m and height 0.7 m. The presence of two length scales in the Karlsruhe experiment makes the comparison with our analysis more difficult, but we can easily compare the results

of the Riga experiment with our “turbulent” (2.33) and “laminar” scalings (2.31), that predict a saturated field of order 10 mT (respectively  $10 \mu\text{T}$ ). Taking into account the qualitative nature of our analysis, we conclude that the “turbulent scaling” is in agreement with the experimental observations whereas the “laminar scaling” predicts a field that is orders of magnitude too small. The “turbulent scaling” also gives a correct order of magnitude for the Karlsruhe experiment if its spatial period is taken as the relevant lengthscale in (2.33). We thus note that the above experiments display a very interesting feature: turbulent fluctuations can be neglected when computing the dynamo threshold; indeed, the observed thresholds are in rather good agreement with those predicted by solving the kinematic dynamo problem for the mean flow alone. However, the high value of  $\text{Re}$  has a very strong effect on the value of the saturated magnetic field above the dynamo threshold.

We emphasize that the correct identification of the dominant transport mechanism of momentum is essential to estimate the order of magnitude of the saturated magnetic field above dynamo threshold. The reason is that it determines the flow distortion by the Lorentz force and thus the saturation mechanism of the field.

A laminar model of the flow thus generally leads to a wrong estimate of the magnetic field amplitude although it sometimes correctly predicts the dynamo threshold. This does not seem to have been fully understood in the early literature on dynamical dynamo models. It is of course possible to recover correct orders of magnitude for the field by using ad hoc turbulent transport coefficients. However, this is not very useful and may even hide the simplicity of the result.

We have shown that a simple scaling law (2.33) for the mean magnetic field generated by laboratory dynamos can be found because they bifurcate from a high Reynolds number flow and operate close to the dynamo onset (Pétréris & Fauve, 2001). It would be interesting to test the validity of this scaling law in existing laboratory experiments. This has not been done yet, but may be achieved both in Karlsruhe and Riga experiments by varying the temperature of liquid sodium and thus its conductivity  $\sigma$ .

## 2.5. EFFECT OF ROTATION

### 2.5.1. WEAK AND STRONG FIELD REGIMES OF THE GEODYNAMO

We first recall some general features displayed by several geodynamo models (for a detailed review, see Chapter 4 and Roberts, 1988). Rotation imposes a strong constraint on the flow that tends to become nearly two-dimensional. The length scale

$\ell$  of the flow in a direction perpendicular to  $\Omega$  is thus much smaller than that along  $\Omega$ ,  $\ell \ll L$ . When convection is generated in a rotating sphere, the flow concentrates in columns of diameter  $\ell \propto L E^{1/3}$ , where  $E = \nu/\Omega L^2$  is the Ekman number (see Chapter 3, and Roberts, 1968, Busse, 1970). This type of flow can generate a large scale magnetic field on length scale  $L$  via an  $\alpha$ -effect (Busse, 1975). Plane layer models (Childress & Soward, 1972; Soward, 1974) display most of the important features of spherical geometries: increasing the rotation rate too much delays the linear instability onset of self-generation because more and more power is necessary to overcome dissipation at small scale  $\ell$ . However, for finite amplitude magnetic fields, the Lorentz force suppresses the rotational constraint and allows large scale motions, leading to much smaller viscous and ohmic dissipation. A subcritical “strong field” branch thus exists below the linear stability onset (St. Pierre, 1993) in addition to the “weak field” branch that bifurcates continuously at the linear dynamo threshold.

Only the weak field branch has been computed analytically, with different models (Childress & Soward, 1972; Soward, 1974; Busse, 1975, 1976). These computations assume the flow to be laminar with a simple geometry. Consequently, the saturated magnetic field is governed by the low Reynolds number scaling (2.31), thus  $\langle |\mathbf{B}|^2 \rangle_{\text{weak}} \propto \rho\nu/\sigma L^2$ . The weak field regime may be stable above the linear threshold (depending on the model) but it becomes unstable for an order one Chandrasekhar number ( $Q = N \text{Re}$ ).

The system then jumps to the strong field regime. It is believed that its scaling corresponds to a balance between the Coriolis and the Lorentz forces (known as the magnetostrophic balance), thus

$$\langle |\mathbf{B}|^2 \rangle_{\text{strong}} \propto \rho\Omega/\sigma. \quad (2.36)$$

For the Earth, taking  $\rho \approx 10^4 \text{ kg m}^{-3}$ ,  $\sigma \approx 3 \cdot 10^5 \text{ S m}^{-1}$  and  $L \approx 3 \cdot 10^6 \text{ m}$ , gives  $B_{\text{weak}} \approx 5 \times 10^{-2} \text{ nT}$  ( $0.5 \mu\text{G}$ ). This is orders of magnitude too small, whereas the strong field scaling,  $\sqrt{\rho\Omega/\sigma} \approx 1 \text{ mT}$  (10 G), looks better.

A very interesting feature of dynamos generated by rapidly rotating flows is thus the subcritical nature of the bifurcation. Consequently, the questions related to the effect of rotation on the linear dynamo threshold are of secondary importance. The mean magnetic energy of finite amplitude dynamo solutions deserves more attention and is strongly affected by rotation.

### 2.5.2. FURTHER COMMENTS ON WEAK AND STRONG FIELD REGIMES

We first note that the form of  $|\mathbf{B}_{\text{weak}}|$  given above is oversimplified. The important aspect is that  $|\mathbf{B}_{\text{weak}}| \rightarrow 0$  if  $\nu \rightarrow 0$  with all other parameters fixed. However, the length scale in the expression of  $|\mathbf{B}_{\text{weak}}|$  is likely to involve both  $L$  and  $\ell \propto LE^{1/3}$ , and thus to be a function of the rotation rate  $\Omega$ . But, note that even if we replace  $L$  by  $\ell$ , we obtain

$$\langle |\mathbf{B}|^2 \rangle_{\text{weak}} \propto \frac{\rho\nu}{\sigma L^2} E^{-2/3}, \quad (2.37)$$

thus changing the field by a factor  $10^5$ . This gives  $5 \mu\text{T}$  (50 mG), which is still too small for the mean field value in the core of the Earth.

As a second step, we may try to incorporate the effect of turbulence since we have already emphasized that it strongly affects the mean magnetic energy. This can be done phenomenologically, starting from the laminar scaling with length scale  $\ell \propto LE^{1/3}$ , and then replacing  $\nu$  by the turbulent viscosity  $\nu_T \propto |\mathbf{u}_T| \ell_T$ , where  $|\mathbf{u}_T|$  is the typical velocity scale on length  $\ell_T$ . In the vicinity of the dynamo threshold, we have  $\text{Rm}_c \approx \mu_0 \sigma |\mathbf{u}_T| \ell_T$ , and we get the turbulent scaling for the magnetic energy with a length scale

$$\ell_T \approx \ell \left( \frac{\text{Rm}_c}{\text{Pm}} \right)^{1/3} = \left( \frac{L}{\mu_0 \sigma \Omega} \text{Rm}_c \right)^{1/3}. \quad (2.38)$$

This gives a more realistic length scale for the diameter of the columns than the laminar one (a few tenth of kilometers rather than a few tenth of meters). We thus obtain a third possible scaling of the magnetic energy

$$\langle |\mathbf{B}|^2 \rangle_{\text{turb}} \propto \frac{\rho\nu}{\sigma L^2} \left( \frac{\text{Rm}_c}{\text{Pm} E^2} \right)^{1/3} = \rho \left( \frac{\Omega^2}{\mu_0 \sigma^4 L^2} \text{Rm}_c \right)^{1/3}, \quad (2.39)$$

giving a more realistic value of the order of a gauss for the mean field.

We finally note that we obtain the strong field scaling from the weak one by replacing  $\nu$  by  $\Omega L^2$ . This only means that, instead of the Stokes term, we have to balance the additional Coriolis term,  $2\Omega \times \mathbf{u}^{(1)}$ , in (2.26) with the Lorentz force. However, such a scaling does not seem to require a subcritical bifurcation. If the Coriolis term is the dominant one, weakly nonlinear perturbation theory will lead to

$$|\mathbf{u}^{(1)}| \propto \frac{|\mathbf{B}^{(0)}|^2}{\mu_0 \rho \Omega L}. \quad (2.40)$$

This gives 
$$\langle |\mathbf{B}|^2 \rangle \propto \frac{\rho \Omega}{\sigma} (\text{Rm} - \text{Rm}_c). \quad (2.41)$$

We obtain the strong field scaling, but without assuming that there is a balance between the Lorentz force and the total Coriolis force. Only the Coriolis force related to the velocity perturbation balances the Lorentz force; this gives the additional term  $Rm - Rm_c$  in the expression of the mean magnetic energy. Although this looks fine, it is not obvious that a perturbative analysis can be worked out that way and we should be cautious in the absence of an explicit analytical example leading to the strong field scaling.

### 2.5.3. SCALINGS OF MAGNETIC ENERGY USING DIMENSIONAL CONSIDERATIONS

The weak field scaling (2.37) gives too small field values but the turbulent (2.39) and the strong field (2.36) ones only differ by roughly an order of magnitude in the case of the Earth. Although their expressions are different, both give possible values of the field for the Earth if we take into account the qualitative nature of our analysis.

It may be interesting to understand the strong field scaling as follows: we already noticed that although magnetic fields exist in a wide range of scales in astrophysics, their values do not seem to be primarily determined by the size  $L$  of astrophysical objects. As a very rough approximation, assume that  $\langle |\mathbf{B}|^2 \rangle$  does not depend on  $L$  and also neglect  $\nu$  since the flow is turbulent (at least at small enough scales). We are then left with 6 parameters,  $B = |\mathbf{B}|$ ,  $\rho$ ,  $\mu_0$ ,  $\sigma$ ,  $U = |\mathbf{u}|$ ,  $\Omega$ , from which we can construct two dimensionless numbers, for instance  $B^2/\mu_0\rho U^2$  and  $Rm Ro = \mu_0\sigma U^2/\Omega$ . We thus get

$$B^2 = \mu_0\rho U^2 g(Rm Ro). \quad (2.42)$$

Close to the dynamo threshold,  $g$  bifurcates from 0 and behaves like  $Rm Ro - (Rm Ro)_c$ , with  $(Rm Ro)_c = \mu_0\sigma U_c^2/\Omega$ . Consequently we obtain

$$B^2 \propto \frac{\rho\Omega}{\sigma} [Rm Ro - (Rm Ro)_c], \quad (2.43)$$

and we recover the strong field scaling. Note that we expect it to be valid if  $Ro \ll 1$  (dominant rotation) but for  $Rm Ro$  large enough to generate the dynamo. We do not expect  $L$  to be the relevant length scale for the strong field regime but the smaller scale  $U_c/\Omega$ . We observe that the flow is turbulent on this scale at dynamo onset ( $U_c^2/\nu\Omega \gg 1$  since  $Re Ro \gg Rm Ro$ ).

## 2.6. SCALING LAWS IN THE LIMIT OF LARGE $Rm$ AND $Re$

Finally, we will consider the case of astrophysical flows where both  $Rm$  and  $Re$  are very large. No laboratory experiments, neither direct numerical simulations being possible in this range of  $Rm$  and  $Re$ , the only way is to try to guess scaling laws for the magnetic field using some simple hypothesis. We thus consider again the minimum set of parameters,  $U, L, \rho, \nu, \mu_0, \sigma$ . We note that discarding global rotation is certainly invalid for most astrophysical objects. However, even in the simplest case of a homogeneous isotropic turbulent flow, with an integral velocity  $U$  in a domain of size  $L$ , no clear-cut result exists neither for the dynamo threshold, nor for the scaling of the magnetic energy. We will shortly review the problem of the dynamo threshold of a turbulent flow and then discuss possible scalings for the magnetic energy.

### 2.6.1. EFFECT OF TURBULENCE ON THE DYNAMO THRESHOLD

Taking into account the minimum set of parameters,  $U, L, \rho, \nu, \mu_0, \sigma$ , dimensional analysis gives for the dynamo threshold  $Rm_c$

$$Rm_c = F(Re). \quad (2.44)$$

For given geometry and large scale flow, the unknown function  $F$  represents how  $Rm_c$  depends on the fluid properties. Finding the behaviour of  $F$  in the limit of large  $Re$  will show how turbulent fluctuations affect the dynamo threshold. This is still an open problem, even in the case of a homogeneous isotropic turbulent flow with zero mean and without helicity. Recent direct numerical simulations show that  $Rm_c$  keeps increasing with  $Re$  at the highest possible resolution without any indication of a possible saturation (Schekochihin *et al.*, 2004). However, if one assumes that the magnetic field is a large scale quantity, i.e. is not affected by the value of viscosity in the limit of large  $Re$  according to the usual phenomenology of turbulence, we immediately get that, if dynamo action is possible in the limit of large  $Re$ , its threshold is given by  $Rm_c \rightarrow \text{constant}$  in this limit.

A lot of work has been performed on the determination of  $Rm_c$  as a function of  $Re$  for turbulent dynamos in the limit of large  $Re$  (or small  $Pm$ ). EDQNM closures have predicted  $Rm_c \approx 30$  for non helical flows (Léorat *et al.*, 1981). The agreement with the above simple argument is not really surprising since these closures keep only the large scales. A lot of analytical studies have been also performed, mostly following

Kazansev's model (Kazansev, 1968). Kazansev considered a random homogeneous and isotropic velocity field,  $\delta$ -correlated in time and with a wave number spectrum of the form  $k^{-p}$ . He showed that for  $p$  large enough, generation of a homogeneous isotropic magnetic field with zero mean value, takes place. This is a nice model but its validity is limited to large  $P_m$  for which the magnetic field has a much larger time scale than the velocity field. In this case, assuming that the velocity field is  $\delta$ -correlated in time is probably a reasonable approximation. However, Kazansev's model has been also extrapolated to large  $Re$ . Various predictions,  $R_{m_c} \propto Re$  (Novikov *et al.*, 1983),  $R_{m_c} \rightarrow \text{constant} \approx 400$  for steep enough velocity spectra ( $p > 3/2$ ) and no dynamo otherwise (Rogachevskii and Kleorin, 1997), or dynamo for all possible slope of the velocity spectrum in the range  $1 < p < 3$  (Boldyrev and Cattaneo, 2004) have been found. These discrepancies result from non rigorous extrapolation of Kazansev's model to large  $Re$ . The calculation is possible only in the case of a  $\delta$ -correlated velocity field in time, and  $\delta(t - t')$ , which has the dimension of time, should then be replaced by a finite eddy turn-over time in order to describe large  $Re$  effects.

A different problem about turbulent dynamos has been considered more recently. It concerns the effect of turbulent fluctuations on a dynamo generated by a mean flow. The problem is to estimate to which extent the dynamo threshold computed as if the mean flow were acting alone, is shifted by turbulent fluctuations. This question has been addressed only recently (Fauve and Pétrélis, 2003) and should not be confused with dynamo generated by random flows with zero mean. It has been shown that weak turbulent fluctuations do not shift the dynamo threshold of the mean flow at first order. In addition, in the case of small scale fluctuations, there is no shift at second order either, if the fluctuations have no helicity. This explains why the observed dynamo threshold in Karlsruhe and Riga experiments has been found in good agreement with the one computed as if the mean flow were acting alone, i.e. neglecting turbulent fluctuations. Recent numerical simulations have shown that in the presence of a mean flow,  $R_{m_c}$  increases with  $Re$  at moderate  $Re$  but then seems to saturate at larger  $Re$  (Ponty *et al.*, 2005).

### 2.6.2. **BATCHELOR'S PREDICTIONS FOR TURBULENT DYNAMO THRESHOLD AND SATURATION**

It may be instructive at this stage to consider the first study on turbulent dynamos made more than half a century ago by Batchelor (1950). Using a questionable analogy between the induction and the vorticity equations, he claimed that the dynamo threshold corresponds to  $P_m = 1$ , i.e.  $R_{m_c} \propto Re$ , using our choice of dimensionless parameters. Pushing the analogy further, he observed that the magnetic field

should be generated mostly at the Kolmogorov scale,  $\ell_K = L\text{Re}^{-3/4}$ , where the velocity gradients are the strongest. He then assumed that saturation of the magnetic field takes place for  $\langle B^2 \rangle / \mu_0 \propto \rho v_K^2 = \rho U^2 / \sqrt{\text{Re}}$ , where  $v_K$  is the velocity increment at the Kolmogorov scale,  $v_K^2 = \sqrt{\nu \varepsilon}$ .  $\varepsilon = U^3/L$  is the power per unit mass, cascading from  $L$  to  $\ell_K$  in the Kolmogorov description of turbulence.

It is now often claimed that Batchelor's criterion  $\text{Pm} > 1$  for the growth of magnetic energy in turbulent flows is incorrect. However, it should be noted that for homogeneous isotropic turbulence without mean flow and helicity, the weaker criterion  $\text{Pm} > \text{constant}$  or  $\text{Rm}_c \propto \text{Re}$ , is still considered to be a possible scenario (Schekochihin *et al.*, 2004). It is thus of interest to determine the minimal hypothesis for which Batchelor's predictions for dynamo onset and saturation are obtained using dimensional arguments.

First,  $\varepsilon = U^3/L$  being the power per unit mass available to feed the dynamo, it may be a wise choice to keep it, instead of  $U$  in our minimal set of parameters, thus becoming  $B, \rho, \varepsilon, L, \nu, \mu_0$  and  $\sigma$ . Then, the predictions of Batchelor can be found using the following simple requirement: let us consider only the dynamo eigenmodes that do not depend on  $L$ . This is a reasonable requirement, since we may hope that in a large domain, there exist some class of small scale magnetic fields which are insensitive to the details of boundary conditions. Then, forgetting  $L$  in our set of parameters, dimensional analysis gives at once  $\text{Pm} = \text{Pm}_c = \text{constant}$  for the dynamo threshold, i.e.

$$\text{Rm}_c \propto \text{Re}. \quad (2.45)$$

We also obtain for the mean magnetic energy density

$$\frac{\langle B^2 \rangle}{\mu_0} = \rho \sqrt{\nu \varepsilon} G(\text{Pm}) = \frac{\rho U^2}{\sqrt{\text{Re}}} G(\text{Pm}), \quad (2.46)$$

where  $G(\text{Pm})$  is an arbitrary function of  $\text{Pm}$ . Close to dynamo threshold, we expect  $G(\text{Pm}) \propto \text{Pm} - \text{Pm}_c$  if the bifurcation is supercritical. Only the prefactor  $\rho U^2 / \sqrt{\text{Re}}$  of (2.46), which is the kinetic energy at Kolmogorov scale, was considered by Batchelor and assumed to be in equipartition with magnetic energy. This class of dynamos being small scale ones, it is not surprising that the inertial range of turbulence screens the magnetic field from the influence of integral size, thus  $L$  can be forgotten. We emphasize that a necessary condition for Batchelor's scenario is that the magnetic field can grow below the Kolmogorov scale, i.e. its dissipative length  $\ell_\sigma$  should be smaller than  $\ell_K$ , thus  $\text{Pm} > 1$ .

### 2.6.3. A KOLMOGOROV TYPE SCALING IN THE LIMIT $Re \gg Rm \gg Rm_c$

The simplest argument in the limit where both Rm and Re are very large is, as usual, to assume that the transport coefficients  $\nu$  and  $\sigma$  become negligible. We are left with one dimensionless parameter and

$$\frac{\langle B^2 \rangle}{\mu_0} \propto \rho U^2. \quad (2.47)$$

We thus obtain equipartition of energy, an assumption often made in the early dynamo literature. The scaling of the mean square magnetic field does not involve the size  $L$  without any further assumption. Note however that this result will not subsist if global rotation is important. The right hand side of (2.47) will then involve an a priori arbitrary function of the Rossby number, thus leading to a possible dependence of  $B$  on  $\Omega$  and  $L$ .

Assuming that the above argument is correct means that the magnetic field is a large scale quantity in the phenomenology of turbulence. There is obviously a strong discrepancy between (2.47) and (2.46). These two laws are the upper and lower limits of a continuous family of scalings that are obtained by balancing the magnetic energy with the kinetic energy at one particular length scale within the Kolmogorov spectrum. It is not known if one of them is selected by turbulent dynamos.

We finally consider the case  $Pm \ll 1$  i.e.  $Re \gg Rm$ . We know from the Karlsruhe and Riga experiments that dynamo action is possible in this range above a moderate value of  $Rm_c$  provided that the mean flow is appropriately chosen. As said above, the problem is still open in the absence of mean flow, although some models predict a much larger but finite  $Rm_c$  in the limit of large Re.

Assuming that a dynamo is generated, we want to give a possible guess for the power spectrum  $|\widehat{B}|^2$  of the magnetic field as a function of the wave number  $k$  and the parameters  $\rho$ ,  $\varepsilon$ ,  $L$ ,  $\nu$ ,  $\mu_0$  and  $\sigma$ . Since  $Re \gg Rm \gg Rm_c$ , the dissipative lengths are such that  $\ell_K \ll \ell_\sigma \ll L$ . For  $k$  in the inertial range, i.e.  $k\ell_\sigma \ll 1 \ll kL$ , we may use a Kolmogorov type argument and discard  $L$ ,  $\sigma$  and  $\nu$ . Then, only one dimensionless parameter is left, and not too surprisingly, we get

$$|\widehat{B}|^2 \propto \mu_0 \rho \varepsilon^{\frac{2}{3}} k^{-\frac{5}{3}}. \quad (2.48)$$

This is only one possibility among many others proposed for MHD turbulent spectra within the inertial range, but it is the simplest. Integrating over  $k$  obviously gives equipartition law (2.47) for the magnetic energy. It is now interesting to evaluate Ohmic dissipation. Its dominant part comes from the current density at scale  $\ell_\sigma$ . We have

$$\frac{\mathbf{j}^2}{\sigma} = \frac{1}{\sigma} \int |\widehat{j}|^2 dk \propto \frac{1}{\mu_0^2 \sigma} \int k^2 |\widehat{B}|^2 dk \propto \frac{\rho}{\mu_0 \sigma} \varepsilon^{\frac{2}{3}} \ell_\sigma^{\frac{2}{3}} \propto \rho \frac{U^3}{L}. \quad (2.49)$$

We thus find that Ohmic dissipation is proportional to the total available power which corresponds to some kind of optimum scaling law for Ohmic dissipation. However, this does not give any indication that this regime is achieved. The discrepancies between plausible laws given in this section show that the problem of turbulent dynamos still deserves a lot of studies.

## 2.7. NONLINEAR EFFECTS IN MEAN FIELD DYNAMO THEORY

Let us now consider the limit of large magnetic Reynolds number  $R_m$ . The majority of research into astrophysical dynamos (see Chapter 6 and Chapter 7) has been performed within the framework of mean field electrodynamics. It can also be a useful approach in geodynamo models (see Section 4.5.1), but here there has also been much recent work on solving the full three dimensional equations (see Section 4.5.3). Mean field electrodynamics, conceived in the 1960's by Steenbeck, Krause and Rädler (see Krause & Rädler, 1980 for full references), is an extremely elegant theory — and is, in many ways, extremely successful. By judicious choice of the various parameters in the theory, it is possible to model a vast range of dynamo-generated magnetic fields (see, for example, the review by Rosner, 2000). It should however always be borne in mind that mean field electrodynamics is a theory of MHD turbulence, and, as in all theories of turbulence (magnetic or non-magnetic), it involves approximations and assumptions. The aim of this chapter is to discuss the various approaches that have been taken towards understanding the nonlinear behaviour of mean field dynamos, concentrating mainly on astrophysical modelling (i.e. high values of the Reynolds numbers  $R_m$  and  $Re$ ). Of particular significance is that the power of present-day computers is now allowing realistic simulations of turbulence — though by no means at the extreme parameter values that pertain in astrophysical situations — and that it is therefore becoming possible to compare theoretical predictions with results from numerical simulations.

The aim of mean field electrodynamics is to provide a mathematical theory for the evolution of magnetic fields on scales large compared with that of the driving turbulent velocity field. Its formulation has already been described in depth in Section 1.5, and so will not be reproduced in detail here. There are though two key points to note, namely:

- (i) that the formulation is essentially linear — being based on the induction equation for given flow statistics, and
- (ii) that, often, progress is possible only for the case of low  $R_m$ . Only in this case

is it possible to make any rigorous statement about the relationship between the fluctuating and mean magnetic fields.

Typically though, astrophysical plasmas are both nonlinear in their behaviour and possess extremely high values of  $Rm$  [ $\mathcal{O}(10^{11})$  in the solar convection zone, for example. See Table IV]. We therefore need to examine just how far the formulation and attendant consequences of mean field electrodynamics can be carried over into the regime of astrophysical relevance.

There are essentially three ways of making progress with understanding the nonlinear evolution of a large-scale magnetic field in a turbulent flow:

- (i) through the incorporation into the mean field formalism of plausible nonlinearities, based on physical arguments;
- (ii) via other MHD turbulence theories, which put the induction equation and momentum equation on an equal footing;
- (iii) via direct numerical simulations of the full governing MHD equations.

In this section, we shall consider each of these areas in turn, and try to give a picture of just where the subject stands at present — to discuss which are the areas of agreement, and which are those of contention. It is intended as an introductory text; it is, deliberately, far from exhaustive, and the work we shall describe has been chosen for illustrative purposes. A much fuller list of references can be found, for example, in the review of galactic magnetic fields by Beck *et al.* (1996) and the recent review of the solar dynamo by Ossendrijver (2003).

For turbulent MHD flows there are two important nonlinearities in the momentum equation. One is the inertial  $(\mathbf{u} \cdot \nabla)\mathbf{u}$  term — the crucial nonlinearity in hydrodynamic turbulence, responsible for energy transfer between different spatial scales; the other is the Lorentz force  $(\mathbf{j} \times \mathbf{B})$ , which provides the back-reaction of the magnetic field on the velocity field. In the following sections, we shall explain how these nonlinearities are accounted for in the three approaches outlined above.

### 2.7.1. NONLINEAR EFFECTS IN THE MEAN FIELD FORMALISM

#### THE INCORPORATION OF PLAUSIBLE NONLINEARITIES

As described in Section 1.5, the standard formulation of mean field electrodynamics leads to a mean induction equation in which the large-scale field evolves under the influence of the tensors  $\alpha_{ij}$  and  $\beta_{ijk}$ , and a large-scale flow (or differential rotation,

$\omega$ ). The simplest means of introducing nonlinear effects into the theory — which are, of course, necessary to prevent unlimited growth of the magnetic field — is to modify one or more of  $\alpha_{ij}$ ,  $\beta_{ijk}$  or  $\omega$  in a manner that reflects the underlying physics. It is though important to point out that such modifications typically do not arise from some self-consistent theory, but are merely physically *plausible*.

For simplicity, let us for the moment consider the case when  $\alpha_{ij}$  and  $\beta_{ijk}$  are isotropic tensors, namely  $\alpha_{ij} = \alpha\delta_{ij}$  and  $\beta_{ijk} = \beta\varepsilon_{ijk}$ ; we need then concern ourselves only with the pseudo-scalar  $\alpha$  and the scalar  $\beta$ . The induction equation for the mean magnetic field  $\mathbf{B}_0$  then takes the form (see Section 1.5.2):

$$\partial_t \mathbf{B}_0 = \nabla \times (\mathbf{U} \times \mathbf{B}_0) + \nabla \times (\alpha \mathbf{B}_0) + \nabla \times [(\eta + \beta) \nabla \times \mathbf{B}_0] . \quad (2.50)$$

At low values of  $Rm$  one may interpret the  $\alpha$ -effect in terms of the physical picture first put forward by Parker (1955), of rising and twisting loops of field giving rise to a mean current anti-parallel to the large-scale field. On physical grounds it is entirely reasonable to argue that this process becomes less effective as the field strength increases — the Lorentz force resisting the tendency to twist field lines — and that therefore  $\alpha$  should be a monotonically decreasing function of the large-scale field  $B_0$ . The most widely used formulation is that proposed by Jepps (1975), with  $\alpha$  taking the form

$$\alpha = \frac{\alpha_0}{1 + B_0^2/\mathcal{B}^2} , \quad (2.51)$$

where  $\alpha_0$  represents the kinematic value of  $\alpha$  and  $\mathcal{B}^2$  represents some reference magnetic energy. At high values of  $Rm$  there is no clear physical picture of even the kinematic (linear)  $\alpha$ -effect, and thus it is not at all surprising that the precise nature of the Lorentz force is much harder to understand. Formulae of the form (2.51) are commonly advanced, but there is considerable controversy over which value of  $\mathcal{B}$  is appropriate.

If  $\alpha$  is “quenched” in the manner suggested by (2.51) one may argue that the turbulent diffusivity  $\beta$  should be similarly reduced, the general argument being that a stronger field resists shredding and hence that the process of turbulent diffusion is inhibited. Dynamo models therefore sometimes adopt a prescription for  $\beta$  of the form

$$\beta = \frac{\beta_0}{1 + B_0^2/\mathcal{B}^2} , \quad (2.52)$$

where the reference energy  $\mathcal{B}^2$  in (2.52) may — or may not — take the same value as in (2.51). There is, of course, a tremendous amount of physics hidden away in the formulae (2.51) and (2.52), and we shall return to this issue in later sections; the aim here however is simply to discuss the general nature of the nonlinearities that are typically incorporated into mean field electrodynamics, and to examine their consequences.

An alternative to (2.51) is to formulate a separate equation for  $\alpha$  — a so-called *dynamic*  $\alpha$ -effect. Schmalz & Stix (1991) postulate that  $\alpha$  may be expressed as the difference between a kinematic and dynamic component,  $\alpha = \alpha_k - \alpha_d$ , where  $\alpha_d$  obeys the relation

$$\partial_t \alpha_d = \mathcal{D}(\alpha_d) + \mathcal{F}(AB), \quad (2.53)$$

where  $\mathcal{D}$  represents a damping term and the function  $\mathcal{F}(AB)$  is chosen to represent the quenching of the  $\alpha$ -effect by the Lorentz force, whilst maintaining the pseudoscalar nature of  $\alpha$ . Yet another possible approach is that of Yoshimura (1978), who argues that the reaction of the field on the driving flow does not occur instantaneously, but only after a certain time  $t_d$  has elapsed. This is built into his formulation of the mean field equations through specifying that  $\alpha$  depends *not* on the magnetic field at the present time  $t$ , but instead on the magnetic field at an earlier time  $t - t_d$ . Such formulations, of either a dynamic  $\alpha$ -effect or an  $\alpha$ -effect that depends on the field at an earlier time, can be justified through rather non-specific physical arguments, as indeed can (2.51); they are though all somewhat arbitrary.

The Lorentz force, via the momentum equation, of course acts not only on the small-scale turbulence — and hence influences the transport coefficients  $\alpha$  and  $\beta$  — but also on the large-scale flow (i.e. on the differential rotation). This can be taken into account through a simple  $\omega$ -quenching model of the form

$$\omega = \frac{\omega_0}{1 + B_0^2/\mathcal{B}^2}, \quad (2.54)$$

based on fairly non-specific arguments that the stress exerted by the small-scale magnetic field inhibits the differential rotation. The large-scale magnetic field also has a *direct* dynamic effect on the large-scale flow; this process, first investigated by Malkus & Proctor (1975), is accounted for by an additional equation for the large-scale velocity.

A third, and rather different, mechanism of dynamo saturation is that due to loss of flux from the region of field generation. This is typically ascribed to an upward escape of flux via magnetic buoyancy, a consequence of the magnetic pressure supporting more gas than would be possible in its absence (see, for example, the review by Hughes & Proctor, 1988). The process is independent of the sign of the magnetic field, and so the simplest prescription is to add a term of the form  $-B^3$  to the right hand side of the mean induction equation (2.50). Again it should be stressed that although this is a reasonable parametrisation, the true physics of magnetic buoyancy instabilities is considerably more complex (see, for example, Hughes, 1991). Indeed, the real picture may be quite subtle; magnetic buoyancy instabilities in a rotating frame — which can lead to an upward transport of magnetic flux — yield helical motions which may, through an  $\alpha$ -effect, be conducive to field generation (see Moffatt, 1978; Thelen, 2000a,b). So magnetic buoyancy may play a *rôle* not only in the loss of field, but also, indirectly, in its generation.

## NONLINEAR MODELS

In modelling a stellar dynamo, the obvious interpretation of the averaging process in the mean-field formulation is as an azimuthal average, leading, in spherical geometry, to equations dependent on radius  $r$ , meridional angle  $\theta$  and time  $t$ . Although less daunting than the full, three-dimensional MHD equations, solution of the axisymmetric mean field equations is still a non-trivial task. It can often therefore be instructive to consider further simplifications. The most drastic is to reduce the governing partial differential equations in  $r$ ,  $\theta$  and  $t$  to a low-order set of ordinary differential equations in  $t$ . One of the earliest such models is that of Weiss, Cattaneo & Jones (1984) who, via a severe truncation of a modal expansion of the mean induction and momentum equations, derived the following seventh order system, which may be regarded as a complex generalisation of the Lorenz equations:

$$\dot{A} = 2D(1 + \kappa|B|^2)^{-1}B - A, \quad (2.55a)$$

$$\dot{B} = i(1 + \omega_0)A - \frac{1}{2}iA^*\omega - (1 + \lambda|B|^2)B, \quad (2.55b)$$

$$\dot{\omega}_0 = \frac{1}{2}i(A^*B - AB^*) - \nu_0\omega_0, \quad (2.55c)$$

$$\dot{\omega} = -iAB - \nu\omega, \quad (2.55d)$$

where  $A$  and  $B$  represent the (complex) poloidal flux function and toroidal field,  $\omega_0$  (real) and  $\omega$  (complex) represent the spatially uniform and spatially varying components of the differential rotation,  $\nu$  and  $\nu_0$  are real constants related to an eddy viscosity. There are three forms of nonlinearity in the above set of equations;  $\alpha$ -quenching in the  $A$  equation, represented through a term of the form (2.51) ( $\kappa$  being a positive real constant), a buoyancy loss term in the  $B$  equation ( $\lambda$  a positive real constant), and the feedback of the Lorentz force on the differential rotation in the  $\omega_0$  and  $\omega$  equations.

Weiss *et al.* (1984) concentrated on the case of  $\kappa = \lambda = 0$ , for which the nonlinear feedback acts only on the differential rotation, and found that solutions of the seventh order system fall into two classes, depending on whether the nonlinear saturation is dominated by  $\omega_0$  or  $\omega$ . The former can be accommodated within the fifth order system obtained by letting  $\nu \rightarrow \infty$ , the latter within the sixth order system formed by letting  $\nu_0 \rightarrow \infty$ . For  $D > 1$  there is an exact nonlinear solution of the seventh order system, corresponding to dynamo waves. For the fifth order system this solution remains stable for all  $D$ ; for the sixth order system, however, it loses stability and more mathematically interesting behaviour ensues. As  $D$  increases, successive Hopf bifurcations, leading to quasi-periodic behaviour, are followed by a period-doubling cascade to chaos. The magnetic field in the chaotic regime has epochs of cyclic activity interspersed with quiescent episodes during which the field amplitude is reduced and varies on a much slower timescale (see Figure 2.1); such behaviour is, of course, suggestive of the time trace of the Sun's magnetic field measured, for example, by the sunspot number.

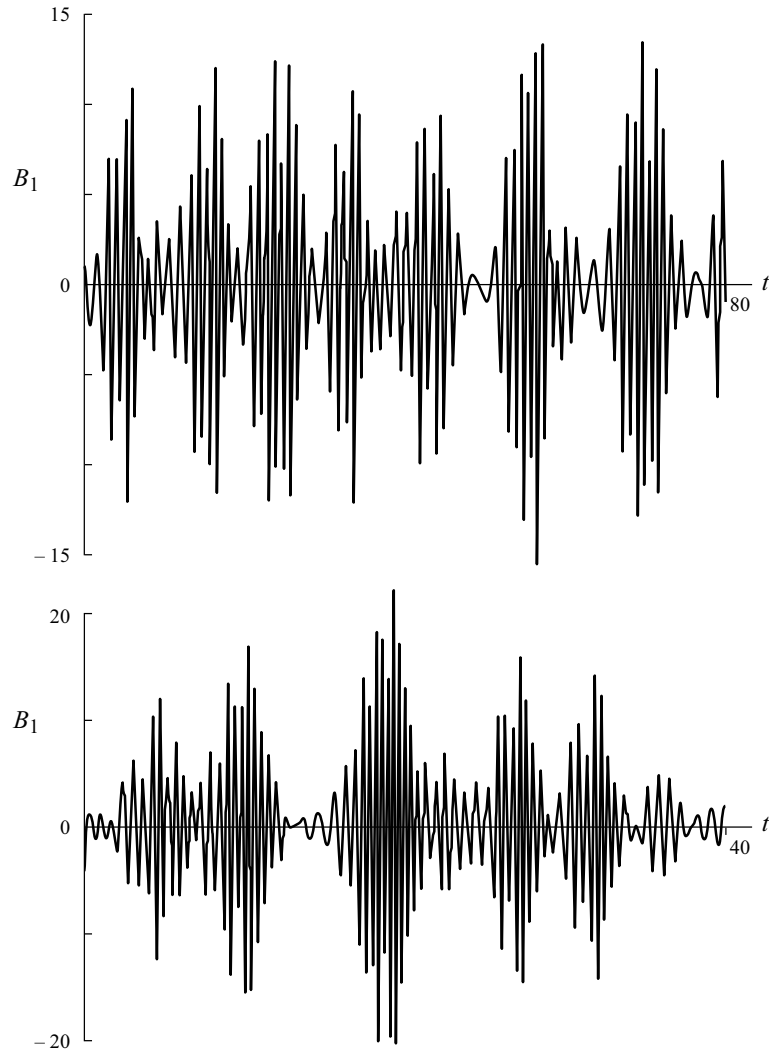


**Figure 2.1** - Aperiodic oscillations of the sixth-order system (derived from (2.55a) – (2.55d) with  $\nu_0 \rightarrow \infty$ ), modulated to give episodes of reduced activity;  $B_1(t)$  (the real part of  $B$ ) for (a)  $D = 8$  and (b)  $D = 16$  (from Weiss *et al.*, 1984).

The natural extension to low-order ODE models — which are local in nature — is to incorporate full spatial variation in one dimension, the most astrophysically relevant way of achieving this being to consider thin-shell dynamos, in which averaging over the radial direction leads to a set of PDEs in  $\theta$  and  $t$ . Such models naturally allow, for example, interactions between the fields in each hemisphere. This approach was adopted by Belvedere, Pidotella & Proctor (1990) who considered a model in which the only manifestation of the Lorentz force is to modify the large-scale velocity. Increases in the dynamo number lead to solutions of increasing spatial and temporal complexity, from simple periodic solutions to quasi-periodic and “pulsed” solutions in which relatively long periods of stasis are interrupted by interludes of cyclic behaviour. The model of Belvedere *et al.* (1990) also allows for the possibility of multiple stable solutions for the same parameter values.

Jennings & Weiss (1991) also considered a one-dimensional model, “flattened” into Cartesian geometry ( $\theta \rightarrow x$ ), governed by the equations

$$\partial_t A = \frac{D \cos x}{1 + \tau B^2} B + \partial_{xx} A, \quad \partial_t B = \frac{\sin x}{1 + \kappa B^2} \partial_x A + \partial_{xx} B - \lambda B^3, \quad (2.56a,b)$$

which may be regarded as a nonlinear modification to (1.114a,b). Their model differs from that of Belvedere *et al.* (1990) not just in the geometry, but also through a different choice of nonlinearities; equations (2.56a,b) contain terms representing  $\alpha$ - and  $\omega$ -quenching and flux loss by magnetic buoyancy, but no direct feedback on the large-scale velocity. Jennings & Weiss (1991) were particularly interested in the phenomenon of symmetry-breaking between the northern and southern hemispheres; via a fairly low-order truncation of equations (2.56a,b), which enabled them to locate both stable and unstable solutions, they were able to construct the bifurcation diagram demonstrating the transitions between dipole, quadrupole and mixed modes. Figure 2.2 shows the bifurcation diagram for the case of  $\kappa = \lambda$ ,  $\tau = 0$ . Of significance is the existence of different types of stable solution (e.g. dipole and quadrupole) at the same value of the dynamo number  $D$ .

Two-dimensional models, in which the variables depend on  $r$  and  $\theta$  (and time) have also received considerable attention, with investigation of all the different types of nonlinearity discussed above (see, for example, Covas *et al.*, 1998, who performed a comparison between algebraic and dynamic  $\alpha$ -quenching). Just as for the models with zero or one spatial dimension a wide variety of behaviour can be found through the incorporation of different nonlinearities.

Equation (2.50), with  $\mathbf{U}$ ,  $\alpha$ ,  $\beta$  and  $\eta$  dependent on (at most)  $r$ ,  $\theta$  and  $t$ , clearly supports non-axisymmetric solutions — with  $\mathbf{B}$  proportional to  $\exp(im\phi)$  in the linear regime. Furthermore it may even be the case that the mode of maximum growth rate is non-axisymmetric. However, one has to exercise a certain amount of caution over the interpretation of non-axisymmetric solutions of (2.50). If the mean-field procedure is that of averaging over the azimuthal angle then — for logical consistency

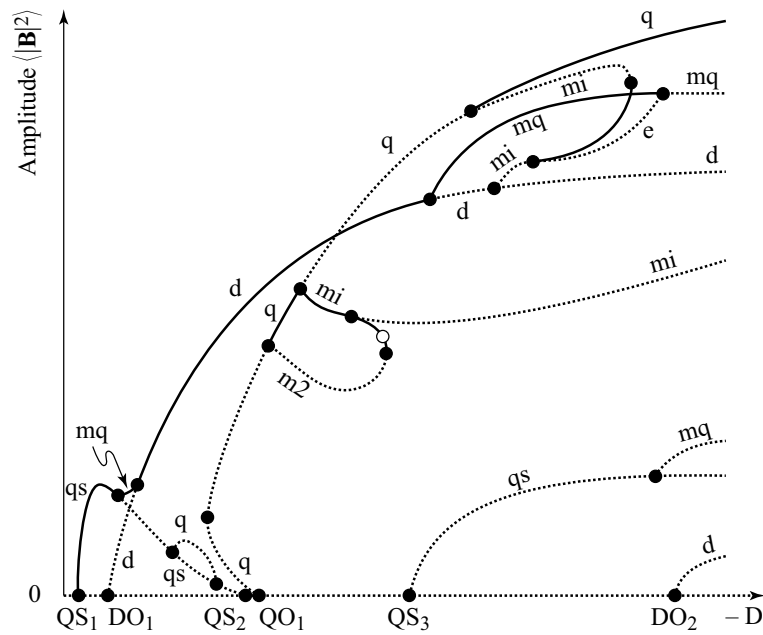


**Figure 2.2** - Bifurcation diagram for the system (2.56a,b) with  $\kappa = \lambda$ ,  $\tau = 0$  and  $D < 0$ ;  $d$ ,  $q$  and  $m$  refer to dipole, quadrupole and mixed mode solutions,  $s$  to steady solutions. Local and global bifurcations are indicated by  $\bullet$  and  $\circ$  respectively (from Jennings & Weiss, 1991).

— the magnetic field in (2.50) must also be axisymmetric. Similarly, an ensemble average — itself somewhat hard to justify for any isolated stellar object — leads to a reduction in the number of spatial dimensions. One other interpretation is that the average represents a filtering between large scales ( $m < m_*$ , say, for some  $m_*$ ) and small scales ( $m \geq m_*$ ) — this allows for the possibility of non-axisymmetric modes of (2.50), but begs the question as to why  $\alpha$  etc. should, in this case, not depend on *all*  $m < m_*$ . Consequently the most consistent interpretation of three-dimensional (non-axisymmetric) solutions of (2.50) is as some sort of temporal average, where  $\partial_t$  represents the rate of change over time scales long compared to that involved in the averaging procedure.

### THE ROBUSTNESS OF NONLINEAR MODELS

Through the choice of the various nonlinearities discussed above, it is possible to obtain a considerable range of solutions to the mean induction equation (2.50), with differing spatial symmetries and a range of temporal complexity, an excellent agreement being possible with observed cosmical fields. The different types of possible solution and their relation to stellar magnetic fields are discussed further in Chapter 6. However, one has to exercise a certain degree of caution in interpreting the results of mean field models. It is well known that the dynamics of low-order systems may be critically dependent on the severe truncation performed to obtain them, and that, for example, chaotic behaviour may disappear in corresponding higher-order systems. Schmalz & Stix (1991) found such a phenomenon in their dynamic  $\alpha$  models. Furthermore, the qualitative behaviour may be sensitively dependent on the precise form of the nonlinearity chosen. Covas *et al.* (1997) re-examined the Schmalz & Stix model by considering different functional forms of the driving term for  $\alpha_d$  in (2.53), and found that significant changes in the chaotic nature of the solutions could result. Tobias (1998) has examined the dependence of dynamo cycle periods on the various nonlinearities that may be included in an interface dynamo model (described in more detail in Section 6.4) and, from the time series of the various models, concluded that it is difficult to discriminate between different nonlinearities.

#### 2.7.2. MHD TURBULENCE THEORIES

The essential principle behind the models discussed in Section 2.7.1 is that the mean induction equation (2.50) is pre-eminent, and that nonlinear effects can be incorporated either through parametrisations of the form (2.51) or through auxiliary equations for  $\alpha$  or  $\omega$ . There are clearly advantages to such an approach; the full horrors of the momentum equation are avoided and, importantly, it appears that most astro-

physical dynamos can, at some level, be modelled in this way. Clearly though, there is always the worry that some of the essential physics of the problem, contained in the momentum equation, is missing. The aim of this section therefore is to review some of the attempts that have been made to model the turbulent dynamo problem through treating the induction and momentum equations on a more equal footing.

One approach is to apply the ideas of mean field averaging not just to the induction equation but also to the momentum equation, on the grounds that the same turbulence occurs in both. On neglecting the magnetic field for the moment, and splitting the velocity field into its mean and fluctuating components,  $\mathbf{U} = \mathbf{U}_0 + \mathbf{u}$ , the (dimensionless) mean momentum equation for an incompressible flow may be written as

$$\partial_t \mathbf{U}_0 + (\mathbf{U}_0 \cdot \nabla) \mathbf{U}_0 = -\nabla P - \nabla \cdot \langle \mathbf{u}\mathbf{u} \rangle + \text{Re}^{-1} \Delta \mathbf{U}_0, \quad (2.57)$$

where the effects of the turbulence are contained in the Reynolds stress tensor

$$Q_{ij} = \langle u_i u_j \rangle. \quad (2.58)$$

Just as in classical mean field electrodynamics, in which the aim is to express the mean e.m.f.  $\mathcal{E} = \langle \mathbf{u} \times \mathbf{b} \rangle$  in terms simply of the mean magnetic field, the aim here is to express the tensor  $Q_{ij}$  in terms of the mean velocity field. This is, however, an even more daunting task than for the induction equation; whereas, at least for weak fields, the latter represents a problem linear in the magnetic field, the momentum equation for fully turbulent flows is inherently nonlinear in the velocity field. The closure of equation (2.57) is thus fraught with even more uncertainties than that of (2.50).

If, however, the assumption is made that  $Q_{ij}$  depends only linearly on the mean part of the velocity field and its first spatial derivatives, then the hydrodynamic analogue of equation (1.103) of Section 1.5.2 may be expressed as

$$Q_{ij} = L_{ijk} U_{0k} - N_{ijkl} \partial_l U_{0k}. \quad (2.59)$$

Furthermore, if the mean flow takes the form solely of a differential rotation, i.e.  $\mathbf{U}_0 = s\omega \mathbf{e}_\phi$ , then (2.59) takes the form

$$Q_{ij} = \Lambda_{ijk} \omega_k - N_{ijkl} \partial_l (\omega \mathbf{e}_\phi \times \mathbf{e}_r)_k. \quad (2.60)$$

The tensor  $\Lambda_{ijk}$  must be symmetric in  $i$  and  $j$ , and hence anisotropic; the first term on the right hand side of (2.60) — the so-called  $\Lambda$ -effect — therefore represents the contribution towards the differential rotation arising from the interaction between global rotation and anisotropic turbulence (Rüdiger, 1989). The second term denotes the contribution stemming from turbulent diffusivity (analogous to  $\beta$  for the mean induction equation). Of course, just as for  $\alpha$  and  $\beta$ , there are no rigorous theories available to calculate  $\Lambda_{ijk}$  and  $N_{ijkl}$ ; these must come from physically plausible,

though to some degree arbitrary, considerations. Mean field dynamos involving the  $\Lambda$ -effect, but with the only nonlinearity that of the large-scale magnetic field on the differential rotation, have been considered by, for example, Brandenburg *et al.* (1991).

The magnetic field though may also influence the differential rotation through modifying, or quenching, the  $\Lambda$ -effect, the turbulent driver of the differential rotation. In the presence of a small-scale magnetic field  $\mathbf{b}$  the total stress tensor becomes

$$Q_{ij}^{\text{tot}} = \langle u_i u_j \rangle - \langle b_i b_j \rangle. \quad (2.61)$$

Formal expressions for  $Q_{ij}^{\text{tot}}$  have been calculated, for a particular turbulence model, by Kitchatinov, Rüdiger & Küker (1994), who also consider the consequences of such a nonlinear  $\Lambda$ -effect for a simple one-dimensional dynamo model. Küker, Arlt & Rüdiger (1999) considered an axisymmetric dynamo model with three different manifestations of the Lorentz force; the Malkus-Proctor mechanism,  $\alpha$ -quenching and  $\Lambda$ -quenching. They found that  $\alpha$ -quenching leads to temporally periodic solutions, whereas the Malkus-Proctor mechanism and  $\Lambda$ -quenching both yield complicated time series with irregular grand minima.

The approach above, couched solely in terms of mean quantities, may be thought of as a one-point closure model. To study small-scale properties for which correlation functions are of crucial importance it is however necessary to consider higher-order moments of the governing equations. Suppose the system of governing equations is written symbolically as

$$\frac{du_i}{dt} + \nu_i u_i = \sum_{jk} M_{ijk} u_j u_k, \quad (2.62)$$

where the  $\{u_i\}$  represent the variables of the system (e.g.  $\{\mathbf{U}, \mathbf{B}\}$  for incompressible MHD), the  $\nu_i$  are the dissipation coefficients, and  $M_{ijk}$  are the nonlinear coupling coefficients (no implicit summation convention is used here). Then, the equation for the two-point correlation function takes the form

$$\frac{d}{dt} \langle u_i u_j \rangle + \nu_i \langle u_i u_j \rangle = \sum_{mn} (M_{imn} \langle u_j u_m u_n \rangle + M_{jmn} \langle u_i u_m u_n \rangle), \quad (2.63)$$

which clearly involves the triple-correlation function. Continuing in this vein leads to an infinite hierarchy of moment equations; to make progress it is therefore necessary somehow to close the system. One of the infinite number of ways in which this may be done — leading to the only MHD turbulence model that has been used to address the dynamo problem — is to adopt what is known as the eddy-damped quasi-normal Markovian approximation (EDQNM), formulated for hydrodynamics by Orszag (1970) and extended to MHD by Pouquet, Frisch & Léorat (1976).

Roughly speaking, closure is achieved by assuming that the joint probability distributions are close to normal, allowing the neglect of all cumulants of order greater than three. An eddy damping, the choice of which allows considerable freedom, is then introduced to determine the decay of the triple correlation, and hence close the system.

From the point of view of mean field dynamo theory, the key result of Pouquet *et al.* (1976) is the derivation of an expression for  $\alpha$  of the form

$$\alpha = -\frac{\tau_c}{3} \left( \langle \mathbf{u} \cdot \nabla \times \mathbf{u} \rangle - \frac{\langle \mathbf{j} \cdot \mathbf{b} \rangle}{\rho} \right), \quad (2.64)$$

where  $\tau_c$  is a typical coherence time of the hydrodynamic turbulence. The result (2.64) provides an extremely appealing description of the saturation of the  $\alpha$ -effect, suggesting that the generation of field through kinetic helicity ( $\langle \mathbf{u} \cdot \nabla \times \mathbf{u} \rangle$ ) is nullified through the manifestation of the Lorentz force through small scale current helicity ( $\langle \mathbf{j} \cdot \mathbf{b} \rangle$ ); as such it has been widely used in studies of nonlinear dynamo action. It is however worth bearing in mind that this is a result born of a number of approximations and assumptions, and it is therefore important to discuss the implications of these. The result may be regarded, in some sense, as the nonlinear extension of the quasi-linear result (1.108), a result that follows from approximating integrals of the form

$$\int_0^\infty \langle \mathbf{u}(\mathbf{x}, t) \cdot \nabla \times \mathbf{u}(\mathbf{x}, t - \tau) \rangle d\tau \quad \text{by} \quad \tau_c \langle \mathbf{u} \cdot \nabla \times \mathbf{u} \rangle. \quad (2.65)$$

However, the nature of the correlation time in MHD turbulence, including its dependence on  $Rm$  and  $B_0$ , remains an important unanswered question (discussed further in the following section). The fact that it is essentially a free parameter of the problem is thus a weakness of the model.

It is also important to consider how the result (2.64) fits in with the classical  $\alpha$ -effect picture, as described in Section 1.5.2. The quasi-linear approximation leads, solely from the induction equation for the fluctuating field, to the expression (1.108) for  $\alpha$ :

$$\alpha = -\frac{\tau_c}{3} \langle \mathbf{u} \cdot \nabla \times \mathbf{u} \rangle. \quad (2.66)$$

However, as discussed by Proctor (2003), the fact that the induction equation remains linear in the magnetic field — even though in the dynamic regime the flow is of course affected by the field — leads formally — even in the nonlinear regime — again to the result (2.66). Any non-linearity will simply be manifested in a change to the kinetic helicity distribution. So what is the origin of the second term in (2.64)? If, instead of the classical picture of  $\mathbf{b}$  being solely dependent on  $\mathbf{B}_0$ , we consider the introduction of a large-scale field  $\mathbf{B}_0$  into a *pre-existing* state of MHD turbulence

with a small-scale velocity  $\mathbf{u}$  and a small-scale field  $\mathbf{b}$  — leading to further perturbations  $\mathbf{u}'$  and  $\mathbf{b}'$  — then, under the quasi-linear approximation, the e.m.f. may be approximated by

$$\mathcal{E} \approx \langle \mathbf{u} \times \mathbf{b}' \rangle + \langle \mathbf{u}' \times \mathbf{b} \rangle. \quad (2.67)$$

Now, using both the induction *and* momentum equations for the fluctuating quantities, the result (2.64) follows (Pouquet *et al.* 1976; Kleeorin & Ruzmaikin, 1982; Gruzinov & Diamond 1994, 1996; Proctor, 2003). It is though vitally important to be clear about the exact meanings of  $\mathbf{u}$  and  $\mathbf{b}$  in this formula.

To obtain a further insight into the  $\alpha$ -effect it is instructive to write  $\mathbf{B} = \nabla \times \mathbf{A}$  and to consider the ideal topological invariant  $\chi = \langle \mathbf{A} \cdot \mathbf{B} \rangle$ , the magnetic helicity (Gruzinov & Diamond, 1994, 1996). From the induction equation, the equations for  $\mathbf{a}$  and  $\mathbf{b}$ , the small-scale fluctuations of the vector potential and the magnetic field, are

$$\partial_t \mathbf{a} = (\mathbf{u} \times \mathbf{B}_0) + (\mathbf{u} \times \mathbf{b}) - \nabla \chi - \eta \nabla \times \mathbf{b}, \quad (2.68a)$$

$$\partial_t \mathbf{b} = \nabla \times (\mathbf{u} \times \mathbf{B}_0) + \nabla \times (\mathbf{u} \times \mathbf{b}) + \eta \Delta \mathbf{b}. \quad (2.68b)$$

Forming the scalar product of (2.68a) with  $\mathbf{b} = \nabla \times \mathbf{a}$ , (2.68b) with  $\mathbf{a}$ , adding, and adopting boundary conditions such that the ensuing surface terms vanish, yields the following equation:

$$\frac{1}{2} \frac{d}{dt} \langle \mathbf{a} \cdot \mathbf{b} \rangle = -\mathbf{B}_0 \cdot \mathcal{E} - \eta \langle \mathbf{b} \cdot \nabla \times \mathbf{b} \rangle \quad (2.69)$$

[see (1.111)], where the angle brackets denote a spatial average and  $\mathcal{E} = \langle \mathbf{u} \times \mathbf{b} \rangle$ . For the case of stationary turbulence we may average over time to obtain

$$\mathbf{B}_0 \cdot \mathcal{E} = -\eta \mu_0 \langle \mathbf{j} \cdot \mathbf{b} \rangle. \quad (2.70)$$

Consequently we have the *exact* result, dependent only on stationarity and suitable boundary conditions, that, for isotropic turbulence

$$\alpha = -\frac{\eta \mu_0}{3 B_0^2} \langle \mathbf{j} \cdot \mathbf{b} \rangle, \quad (2.71)$$

[cf. (1.112)], where  $\mathbf{b}$  is the *entire* small-scale magnetic field and where angle brackets here are to be understood as denoting a space *and* time average. The result (2.71) though involves the small-scale field and current, whereas a true mean field theory must involve only large-scale variables. One approach to eliminating the small-scale behaviour is to equate the two expressions for  $\langle \mathbf{j} \cdot \mathbf{b} \rangle$  from (2.64) and (2.71) (Gruzinov & Diamond, 1994), thereby leading to what is known as the formula for strong (or even “catastrophic”) suppression,

$$\alpha = \frac{\alpha_0}{1 + \text{Rm} (B_0^2 / \mu_0 \rho) / \langle \mathbf{u}^2 \rangle}. \quad (2.72)$$

It is though worth reiterating the different natures of the expressions (2.71) and (2.64). In expression (2.71) — which is *exact* —  $\mathbf{b}$  refers to the total small-scale field, whereas in (2.64) — which is only an approximate result — it refers to a pre-existing small-scale field.

The astrophysical consequences of (2.72), if it is correct, are highly significant in that it implies that the  $\alpha$ -effect ceases to be effective at an extremely low value of the large-scale magnetic field (see Vainshtein & Cattaneo, 1992). This issue, which remains very controversial, is now also being addressed through numerical simulations, described in the following section. We shall therefore delay further discussion of (2.72) to the following section.

### 2.7.3. DIRECT NUMERICAL SIMULATIONS

It is worth stating, from the outset, that direct numerical simulations cannot provide a complete answer to the astrophysical dynamo problem; it is simply not possible to solve the governing equations at the extreme parameter values ( $Re \gg 1$ ,  $Rm \gg 1$ ) that pertain astrophysically. With the most powerful computational facilities now available, it is feasible to simulate flows with  $Re \approx Rm \approx 10^3$  and that possess a reasonable scale separation between that of the driving flow and the largest scale available to the magnetic field. However, given that spatial resolution increases, in each direction, as the inverse square root of the dissipation, and also that the time step decreases in inverse proportion to the resolution, a comparable calculation with  $Re \approx Rm \approx 10^9$  requires  $10^{12}$  times as many operations. Even with a doubling in computer speed every few years we are clearly nowhere near being able to solve the full problem merely by what Roberts & Soward (1992) term the “brute force” approach. Indeed, even a truly realistic *simulation* of a physical process does not, of itself, constitute a true *understanding* of the process. That said, a computational approach, properly used, can help us to gain an understanding of nonlinear MHD processes, can verify — or refute — existing theories, and can help point the way to new theoretical approaches.

The most ambitious global models of stellar dynamos remain those of Glatzmaier (1985a,b), who investigated self-consistent (i.e. nonlinear) dynamo action driven by thermal convection in a rotating spherical shell. Glatzmaier considered the case of an anelastic gas, thereby filtering out short time scale sound waves whilst retaining the effects of a large density stratification, following on from earlier Boussinesq models of Gilman & Miller (1981) and Gilman (1983). Glatzmaier’s models employed subgrid-scale eddy diffusivities, but otherwise contained essentially no parametrisation. In particular, there was no freedom to specify  $\alpha$  or  $\omega$ ; these simply emerged, as properties of the convective motions, through a self-consistent solution of the governing equations. Glatzmaier (1985a) considered the case of an every-

where superadiabatic atmosphere; for the parameter values adopted he found that the convection took the form of north-south rolls, as suggested by the Proudman–Taylor theorem for rapidly rotating fluids, with the angular velocity decreasing with increasing latitude at the surface. The magnetic field was antisymmetric about the equator (as for the Sun) but, unlike the Sun, was found to propagate towards the poles. This is sometimes viewed as a failure of the model, in that it differs in this respect from the observed solar field. It is though, as discussed earlier, not practicable to model the Sun in terms of adopting realistic parameter values, and it is (even now) premature to expect self-consistent models that reproduce solar features. The simulations of Glatzmaier represent an extremely important success, demonstrating conclusively the feasibility of a nonlinear dynamo *with minimum parametrisation* (see also the discussion in Section 4.5). Glatzmaier (1985b) did address the question of the direction of propagation of the field, by undertaking a further calculation with a different convective stratification, with the outer two thirds (in radius) superadiabatic and the inner third subadiabatic, the premise being that the helicity and differential rotation in the region of overshooting convection would be such as to drive the dynamo waves towards the equator. The results suggested that this may be the case, but were inconclusive, suffering from the lack of numerical resolution in the inner half of the shell.

Since the studies by Glatzmaier — and in contrast to the path pursued in modelling the geodynamo — attention has shifted away from direct numerical simulations of the entire global dynamo process in a spherical geometry, either towards local, Cartesian models of nonlinear dynamos, or towards “stripped down” simulations aimed at understanding isolated specific aspects of the dynamo mechanism. The former avenue has been pursued by Brandenburg and his co-workers, who have investigated both convectively driven dynamos (Brandenburg *et al.* 1996) and dynamos driven by helical forcing (Brandenburg 2001). The latter approach has been aimed principally at obtaining a more complete understanding of the nonlinear behaviour of the transport coefficients  $\alpha$  and  $\beta$  in a turbulent flow at high Rm; for example, does formula (2.51) correctly describe the saturation of  $\alpha$  and, if so, what is the appropriate value for  $B^2$  at which the energy of the large-scale field becomes significant? Cattaneo & Vainshtein (1991) considered the (guaranteed) decay of a co-planar, large-scale field in two-dimensional turbulence, in order to calculate the dependence of the turbulent diffusivity on the strength of the large-scale field  $B_0$ . With  $\text{Rm} = \mathcal{O}(10^2)$ , and by varying  $B_0$ , they found that the decay of the field could be considered to be kinematic only for extremely weak fields, with  $B_0^2 \lesssim \langle \mathbf{u}^2 \rangle / \text{Rm}$ , and that the turbulent magnetic diffusion time for a large-scale field of characteristic length  $L$  is well-represented by the formula

$$\tau_T (= L^2/\beta) = \frac{L^2}{\eta} \left( \frac{1}{\text{Rm}} + \frac{1}{M^2 + 1} \right), \quad (2.73)$$

where  $M$  is the Alfvénic Mach number, the ratio of the flow speed to the Alfvén speed of the large-scale field. The key physical process behind the suppression of turbulent diffusion is that the field becomes strong (i.e. of equipartition strength) on the scale of the flow whilst remaining weak at large scale, with  $\langle |\mathbf{B}|^2 \rangle \approx \text{Rm} B_0^2$ . The strong small-scale field resists the rapid deformation necessary for turbulent diffusion, which is thus inhibited. Alternatively, one may consider the problem from a Lagrangian perspective, based on the ideas of Taylor (1921). Turbulent diffusion is achieved by the exponential separation of fluid particle trajectories; the presence of a strong small-scale field provides the fluid particle with a long-term “memory” — their separation is inhibited and the diffusion reduced (Cattaneo, 1994). Clearly any correlation time will be dependent on the magnetic field, and this needs to be brought out in models of MHD turbulence.

The two-dimensional diffusion problem is though rather special, for a number of reasons. Geometrically, there is no possibility of interchange motions, which can bring together oppositely directed field lines without bending them — this suggests that any suppression of diffusion for three-dimensional flows should be weaker. Furthermore, in two dimensions, field decay is guaranteed (Zeldovich’s (1957) theorem), following from the fact that the one component of the magnetic potential satisfies the heat equation. The question of the suppression (if any) of the turbulent magnetic diffusivity for general, three-dimensional flows remains completely open. It is an extremely difficult question to attack numerically, for two reasons. One is simply a question of computational resources, in that one needs to accommodate a magnetic field that varies on a large scale whilst still resolving the small-scale turbulence. The second, and more difficult, problem is conceptual, arising from the fact that turbulent three-dimensional flows are almost certainly small-scale dynamos at sufficiently high  $\text{Rm}$  and, for flows lacking reflectional symmetry, may be large-scale dynamos also. It is thus not a straightforward matter to determine how the *rôle* of  $\beta$  should be disentangled from that of field amplification.

Calculating the  $\alpha$ -effect numerically is more clear-cut since it can be determined unambiguously by measuring the correlation in a turbulent flow between an imposed *uniform* magnetic field and the resulting e.m.f.,  $\langle \mathbf{u} \times \mathbf{b} \rangle$ . Such calculations are not dynamo simulations — since they have an imposed field with non-zero mean — but are aimed at addressing the one particular issue of the nonlinear nature of the  $\alpha$ -effect. Cattaneo & Hughes (1996) and Cattaneo, Hughes & Thelen (2002) have investigated forced helical, incompressible turbulence, in the presence of an imposed mean field  $B_0$ , in order to measure the dependence of  $\alpha$  on  $\text{Rm}$  and  $B_0$ . As for the case of  $\beta$  in two dimensions,  $\alpha$  is quenched at very weak values of  $B_0$ , the results being approximated by a formula of the form

$$\alpha = \frac{\alpha_0}{1 + \text{Rm}^\gamma (B_0^2 / \mu_0 \rho) / \langle \mathbf{u}^2 \rangle}, \quad (2.74)$$

for some  $\mathcal{O}(1)$  constant  $\gamma$  (see Figure 2.3). The physics behind the suppression of  $\alpha$  can be understood, at least in a rather general manner, in an analogous fashion to the suppression of  $\beta$ ; namely that a weak large-scale field gives rise, for large  $R_m$ , to a very strong small-scale field which inhibits  $\alpha$ . It should be pointed out that this is a more subtle issue than simply a reduction in kinetic helicity; Cattaneo & Hughes (1996) showed that a suppression of  $\alpha$  by a factor of order  $R_m$  is achieved with only a halving of the kinetic helicity. Clearly — as for diffusion — it must be tied to the ideas of the fluid particles becoming imbued with a “memory”. However, the micro-physics underlying  $\alpha$  at high  $R_m$  is not at all well understood, even in the kinematic regime. A formal analysis of the case of perfect electrical conductivity ( $R_m$  infinite) leads to the following expression for  $\alpha$  in terms of the Lagrangian displacement  $\xi$  (Moffatt, 1974):

$$\alpha = -\frac{d}{dt}\langle \xi \cdot \nabla \times \xi \rangle, \quad (2.75)$$

and one may speculate that a reduction in the separation of fluid trajectories will lead to a reduction in the average in (2.75). There are though doubts as to the validity of (2.75) even in the kinematic regime for large but finite  $R_m$  and certainly, at the moment, there is no proper theory of the suppression of  $\alpha$  when  $R_m$  is large. The whole issue of the nonlinear behaviour of the transport coefficients of mean field theory is discussed at much greater length in the recent review by Diamond, Hughes & Kim (2004).

As mentioned above, the result (2.74), assuming that it carries through to the astrophysical  $R_m$  regime, poses a severe problem for the generation of large-scale fields, in that it implies that the  $\alpha$ -effect ceases to be effective once the energy of the large-scale field becomes comparable to the equipartition energy divided by  $R_m$ . As such, the result has been criticised, although in a somewhat time-dependent and self-contradictory fashion. Field, Blackman & Chou (1999) claimed that the strong suppression result (2.74) was incorrect, despite its excellent agreement with numerical experiments, but gave no indication as to where they thought the error lay. In a later work, Blackman & Field (2000) underwent an abrupt change of direction, arguing instead that the result was, after all, correct, but was inapplicable to astrophysical situations, their argument being that the dynamics would be dominated by the flux of magnetic helicity through the boundaries, a quantity that is of course zero in periodic domains, such as used by Cattaneo & Hughes (1996). It is indeed true that a formal derivation of the  $\alpha$ -effect, via manipulation of equations (2.68a) and (2.68b), leads to the presence of surface terms in the expression for  $\alpha$  (i.e. extra surface terms in equations (2.69) and (2.70)) — terms which vanish not only for periodic boundary conditions but also for a number of choices of reasonable boundary conditions. What is totally unclear though is the importance of such terms in an astrophysical context. The issue of  $\alpha$ -suppression therefore remains a controversial and important topic.

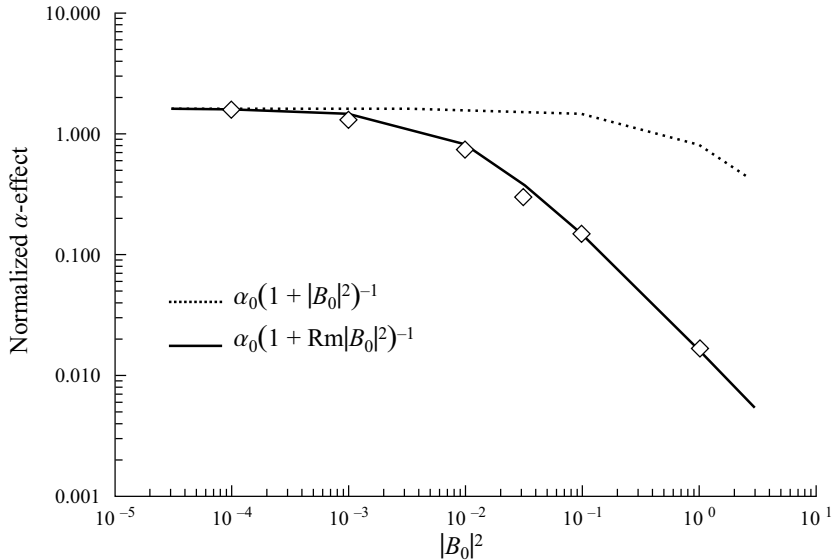


**Figure 2.3** - The results of numerical simulations (diamonds) determining  $\alpha$  in a forced, helical, chaotic flow, and their relation to two competing theoretical results (from Cattaneo & Hughes, 1996).

The aim of this section has been to give an introduction to what, broadly speaking, are the three possible approaches to understanding the behaviour of nonlinear large-scale dynamo action. (The issue of the nonlinear evolution of small-scale dynamos, in which the field exists on scales comparable with or smaller than that of the driving velocity, is also a fascinating and relevant topic, though beyond the scope of this review.) Each has its strengths and weaknesses. Parametrisations of mean field theory, of the sort discussed in Section 2.7.1, are computationally tractable and thus allow an in-depth study of the dependence of a particular model on the governing parameters. Signatures of stellar magnetic fields — such as the solar butterfly diagram — can be faithfully reproduced through parametrised mean field models. The drawback of such models comes though from the somewhat arbitrary choice of parametrisation and the difficulties in assigning particular behaviour to specific physical causes. As such, one must be very careful in asserting that astrophysical magnetic fields can really be *understood* on the basis of such models, and even more careful before making predictions about future magnetic behaviour. Theories of MHD turbulence (such as the EDQNM model discussed above) have their roots more firmly attached to the Navier-Stokes equation, but still rely on a number of assumptions in order to obtain a tractable set of governing equations. It is in formulating these assumptions that all the difficulties arise. Numerical approaches, on the other hand, are able to solve the full nonlinear governing equations, without approximation, but — even with the most powerful computational facilities currently available — only in

parameter regimes still far removed from those that describe most astrophysical phenomena. Given all these drawbacks, what is the best hope for progress? Probably the most promising avenue is to improve our understanding of specific, rather narrowly defined questions — such as, for example, the dependence on  $Rm$  and  $B_0$  of  $\alpha$  and  $\beta$  — via bespoke computational models, and then to incorporate these findings into improved turbulence theories. Today’s massively parallel computers are able to model turbulent flows at moderate (from an astrophysical view) values of the Reynolds numbers; from such models we must seek scalings and other information to lead us into the true astrophysical regime. It is a fascinating though formidable challenge.

## 2.8. PHYSICALLY-REALISTIC FARADAY-DISK SELF-EXCITED DYNAMOS

In this final section we will highlight how nonlinearities can yield a chaotic dynamical behavior of dynamo action by returning to the matter of disk dynamos introduced in Section 1.2.1.

Self-excited dynamos are nonlinear electro-mechanical engineering devices or naturally-occurring magnetohydrodynamic (MHD) fluid systems such as the “geodynamo” operating within the Earth’s liquid metallic outer core (see Chapter 4), that through the action of motional induction convert mechanical energy into magnetic energy without the involvement of permanent magnets. Owing to the intractability of the governing nonlinear *partial* differential equations (PDEs) in four independent variables (space and time) in the investigation of generic nonlinear processes in such dynamos it is not yet possible to exploit numerical models of MHD systems now being developed by various groups. As a research strategy these processes are better studied in the first instance by analysing the more tractable nonlinear *ordinary* differential equations (ODEs) in just one independent variable (time) that govern the behaviour of simpler systems, such as electro-mechanical devices based, for example, on a steadily forced Faraday disk dynamo.

In this section we summarise the main findings of recent mathematical investigations of the simplest imaginable Faraday disk dynamo systems that are both physically realistic and provide a basis for investigating generic nonlinear effects MHD dynamos.

Unlike most systems discussed in the extensive literature on disk dynamos, the governing equations take into account the re-distribution of kinetic energy within the system by Lorentz forces, and the equations are “structurally stable” because they include, in addition to terms representing dissipation due to ohmic heating equally-

crucial terms representing mechanical friction. Over wide ranges of conditions these forces give rise to “nonlinear quenching” of dynamo fluctuations, a process which has already been invoked by one of us (RH) as the basis for explaining possibly the most striking feature of the long-term behaviour of the main geomagnetic field, namely “superchron” intervals as long as 30 Ma when the polarity reversals disappear from the palaeomagnetic record (see Chapter 4).

### 2.8.1. HISTORICAL SURVEY

In the 1860’s, three decades after Faraday’s invention of a dynamo incorporating a stationary permanent magnet, Varley, Wheatstone and von Siemens independently conceived and applied the self-excitation principle, replacing the permanent magnet of the Faraday dynamo with a stationary coil through which the dynamo current could be diverted. Mathematical models of self-excited homopolar dynamos, which came much later, have been analysed (mainly) by theoretical geophysicists and astrophysicists interested in low-dimensional analogues of MHD self-excited dynamos.

These mathematical investigations began in the 1950’s with the pioneering work of Bullard and Rikitake. Bullard treated the simplest-imaginable case of all (as introduced in Section 1.2.1), when (see below for full explanations of the various parameters):

- (a) there is no motor in the system [corresponding to  $H = 0$ , so that the  $\omega$  together with (2.77d) are therefore redundant];
- (b) the disk resistance  $\hat{R}$  is infinite (so that  $\hat{I}$  and equation (2.77b) are redundant);
- (c) mechanical friction retarding the motion of the disk is negligible [so that  $K = 0$  in (2.77c)].

By coupling two Bullard-type systems together, Rikitake introduced the much-studied two-disk dynamo system governed by an autonomous set of three nonlinear ODEs, the minimum number for chaotic solutions to be possible.

The neglect of mechanical friction seemed at the time to be a reasonable assumption to make, but it is now known that the assumption has the unfortunate consequence of rendering the equations governing the original Bullard and Rikitake systems structurally unstable and their solutions, except as transients, physically unrealistic (see Hide, 1995, and Moroz *et al.*, 1998a).

In the original Bullard (1955) dynamo  $\check{\alpha}$  is the only non-zero control parameter, for there is no series motor, the disk conductance is zero and the sliding contacts at the

rim and axle of the disk are assumed to be frictionless. Persistent solutions are found with characteristics that depend on  $\tilde{\alpha}$  and the initial conditions. They represent periodic (but non-harmonic) relaxation oscillations in which the dimensionless electric current generated in the system,  $x$ , never changes sign.

The long-held view (see Rikitake, 1966) that the addition of mechanical friction [in our notation (2.81b),  $\tilde{\kappa} \neq 0$ ] would make no qualitative difference to this behaviour is untenable. Hide (1995) has shown that the mathematical equations governing the Bullard single-disk system, as well as all other friction-free multiple-disk dynamo systems based upon it [including the influential Rikitake (1958) double-disk system], are “structurally unstable”. In the presence of mechanical friction the Bullard system eventually becomes steady after initial transients have died away (see also Moroz *et al.*, 1998). When friction is weak these transients certainly resemble ‘friction-free’ fluctuations, notably periodic Bullard-type non-reversing fluctuations in the single-disk case and Rikitake-type chaotic fluctuations with reversals, but they die away. It is noteworthy however that persistent chaotic fluctuations with reversals can occur in a Rikitake system consisting of two coupled identical Bullard dynamos when mechanical friction is added, provided that the two coefficients of mechanical friction are not the same (Ershov *et al.*, 1989; see also Hide, 1997a, and Moroz *et al.*, 1998).

Noting that dynamo action is impossible in the limiting case when the electrical resistance of the disk vanishes (for the magnetic flux linkage of a perfect conductor cannot change) Moffatt (1979) extended the Bullard (friction-free) model by considering the case of non-zero disk conductance, thereby allowing eddy currents to flow. This is the case when, in addition to  $\tilde{\alpha}$ , the control parameters  $\xi$ ,  $\chi$  and  $\tilde{\nu}$  required to specify the electrical properties of the disk are also non-zero.

When mechanical friction in the disk is also taken into account, so that  $\tilde{\lambda} \neq 0$ , we have the case analysed in detail by Knobloch (1981) and later by Plunian *et al.* (1998), who also treated a double-disk system, thereby extending the Ershov study to cases of non-zero disk conductance.

In the Knobloch (1981) case, the governing equations are transformable into the celebrated Lorenz set, which can of course have chaotic solutions. We note here that Malkus (1972; see also Robbins, 1976) realised that by adding an electrical shunt to the Bullard system and taking mechanical friction into account he could obtain governing equations of the Lorenz type.

Hide *et al.* (1996) extended the Bullard system by placing a capacitor in series with the coil and including mechanical friction in the disk and then demonstrated the mathematical equivalence of this system to one obtained by replacing the capacitor with a linear motor, with (unavoidable) mechanical friction in the motor equivalent to (unavoidable) leakage resistance in the capacitor.

### 2.8.2. CHARACTERISTICS OF SELF-EXCITED DYNAMOS

The salient characteristics of all self-excited dynamos can be summarised as follows (Hide, 2000):

- (a) the mechanical-to-magnetic energy conversion process is due to motional induction (represented in the equations governing MHD dynamos by the nonlinear motional induction term  $\mathbf{u} \times \mathbf{B}$ , where  $\mathbf{u}$  denotes the Eulerian flow velocity at a general point and  $\mathbf{B}$  the magnetic field), and it starts with the amplification of any infinitesimally weak adventitious magnetic field;
- (b) for the amplification process to work, motional induction must overcome ohmic losses, implying that the electrical resistance of the system must be sufficiently low (in MHD dynamos this means a sufficiently high magnetic Reynolds number—defined as the product of a characteristic flow speed, a characteristic length, the magnetic permeability of the fluid, and its electrical conductivity);
- (c) for the magnetic field to diffuse into the surrounding medium, the electrical resistance must not be *too* low and this sets an *upper* limit on the magnetic Reynolds number in MHD dynamos;
- (d) ponderomotive (Lorentz) forces (as represented by the nonlinear term  $\mathbf{j} \times \mathbf{B}$  in MHD dynamos, where  $\mathbf{j}$  is the electric current density) re-distribute kinetic energy within the system (thereby retarding the buoyancy-driven eddies in typical MHD dynamos such as the geodynamo and accelerating motions in other parts of the eddy spectrum);
- (e) no matter how weak, mechanical friction viscosity in MHD dynamos, which *inter alia* dissipates kinetic energy, is never negligible;
- (f) internal coupling and feedback (as represented by the terms  $\mathbf{u} \times \mathbf{B}$  and  $\mathbf{j} \times \mathbf{B}$  in MHD dynamos) give rise to behaviour characteristic of nonlinear systems, i.e. sensitivity to initial conditions leading to non-uniqueness (sometimes called “multiple solutions”), large amplitude fluctuations (including “deterministic chaos”), hysteresis, nonlinear stability, etc.

A strategy advocated in Hide (2000) for discovering generic processes in self-excited dynamos is to start by investigating the temporal behaviour of simple (but not oversimplified) systems, such as Faraday disk homopolar generators, governed by tractable *ordinary* differential equations (ODE’s) in the single independent variable time,  $T$  (say), and then, in the light of the results thus obtained, formulating and executing suitable diagnostic tests of less tractable MHD systems governed by nonlinear *partial* differential equations (PDE’s), in four independent space-time variables. Apart

from the undoubted mathematical interest of the solutions of the governing ODE's, the findings of those investigations that treat physically-realistic systems –and we must emphasise here this requirement excludes all the friction-free systems that have been treated in the literature (Hide, 1995) including the much-discussed pioneering studies of Bullard (1955) and Rikitake (1958), *cf.* characteristic (e) above– provide general insights into the likely behaviour of the more complex MHD systems, such as the geodynamo operating within the Earth's liquid metallic outer core.

In hydrodynamics the governing mathematical equations express the laws of mechanics and thermodynamics, to which the laws of electrodynamics must be added in the case of MHD. The equations owe their nonlinearity largely to advective terms such as  $(\mathbf{u} \cdot \nabla)\mathbf{u}$ ,  $(\mathbf{u} \cdot \nabla)\mathbf{B}$ ,  $(\mathbf{B} \cdot \nabla)\mathbf{u}$ ,  $(\mathbf{B} \cdot \nabla)\mathbf{B}$ , etc., which can in some circumstances promote order and stability, as in the case of solitons and in others disorder, instability and sensitivity to initial conditions.

In mathematical analyses, such sensitivity can give rise to multiple solutions associated with “unfoldings” in phase space near co-dimension-two bifurcations, so that steady solutions are able to co-exist at the same point in “control parameter” space with oscillatory and chaotic solutions. In laboratory (and numerical) work sensitivity to initial conditions is manifested as non-uniqueness, chaos, and hysteresis at regime transitions found, for example, in experiments on sloping convection (see e.g. Hide *et al.*, 1994) and Taylor-Couette flow (see e.g. Fenstermacher *et al.*, 1979).

### 2.8.3. GOVERNING EQUATIONS IN DIMENSIONAL FORM

A Faraday disk homopolar dynamo system which satisfies all the criteria listed above comprises a single disk and coil arrangement with a crucial additional element in the circuit, namely an electric motor with torque characteristics that are not necessarily linear connected in series with the coil (Hide, 1997a, 1997b), see Figure 2.4. The motor enables Lorentz forces to re-distribute kinetic energy within the system, where feedback and coupling also contribute to its nonlinear characteristics.

The disk is driven into rotation with angular speed  $\Omega(T)$  by a steady applied couple  $G$ , where for the rest of this chapter  $T$  denotes dimensional time. Retarding the motion of the disk is a frictional couple  $-K(T)$  as well as a Lorentz couple  $-I(MI + \widehat{L}\widehat{I})$ . Here  $I = I(T)$  is the main electric current generated by the dynamo and  $\widehat{I}(T)$  is the eddy current circulating azimuthally in the plane of the disk (hereafter just “eddy current”), that is induced when  $dI/dT \neq 0$ . The factor  $(MI + \widehat{L}\widehat{I})$  thus represents the magnetic flux linkage of the disk if  $2\pi M$  is the mutual inductance between the disk and coil and  $2\pi\widehat{L}$  is the self inductance of the disk. In the absence of Lorentz forces, friction alone retards the motion of the disk, and when  $G$  is steady –the case of interest here– the disk rotates with steady angular speed

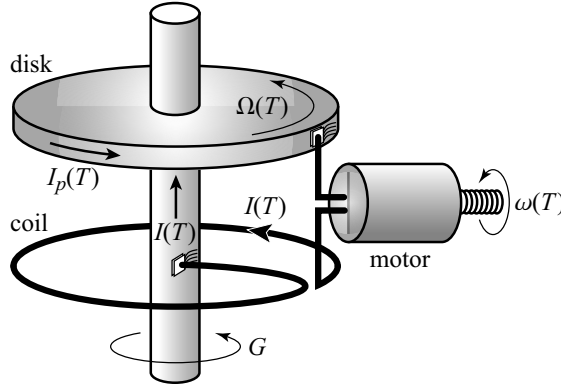


**Figure 2.4** - Single-disk dynamo with nonlinear series motor (*cf.* Hide, 1997a,b).

$$\Omega = G/K.$$

The armature of the motor is driven into rotation with angular speed  $\omega$  relative to the stationary ambient magnetic field within the motor by a Lorentz couple  $HIf(I)$ , in general a quadratic function of  $I$ , produced by the dynamo current, and it is retarded by a linear frictional couple  $-D\omega$ . Here  $H$  is such that  $Hf(I)\omega$  is the back e.m.f. due to the presence of the motor in the dynamo circuit [see equation (2.77a) below], where

$$f(I) = (1 - \varepsilon) + \varepsilon SI, \quad (2.76)$$

and  $0 \leq \varepsilon \leq 1$ .  $f(I)$  specifies the stationary ambient magnetic field within the motor and depends on the design of the motor. The parameter  $\varepsilon$  measures the nonlinearity of the motor's electro-mechanical characteristics, which vanishes only in the special case when  $\varepsilon = 0$ . The contribution to the stationary field  $\propto \varepsilon SI$  is produced by diverting the dynamo current through stationary field windings ( $S$  being a measure of the mutual inductance between the armature and the field windings). This is complemented by the contribution proportional to  $(1 - \varepsilon)$  provided by an "outside source".

From a geophysical and astrophysical point of view it is important here to note that this outside source need not necessarily be a permanent magnet, for the magnetic field produced by the current in the coil of a second dynamo would do just as well (see Hide, 2000).

It will be convenient in this section to use the term "linear motor" when  $\varepsilon = 0$  and "nonlinear motor" when  $0 < \varepsilon \leq 1$  (unless otherwise stated), and also to distinguish two sub-classes of nonlinear motor, namely "quadratic motor" when  $0 < \varepsilon < 1$  and "square motor" when  $\varepsilon = 1$ .

The governing 4-mode dimensional set of nonlinear ODE's in the  $(I, \Omega, \omega, \hat{I})$  is

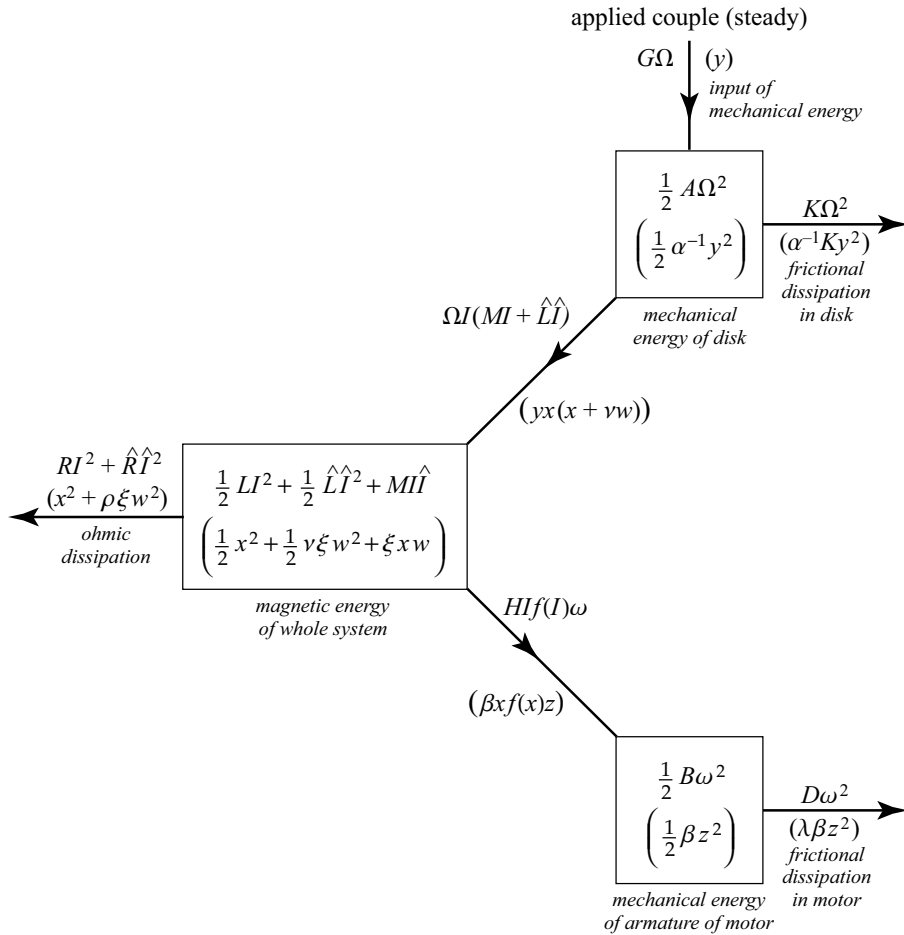


**Figure 2.5** - Energetics of the single-disc dynamo with nonlinear series motor.

given by (see Hide, 1998)

$$L \frac{dI}{dT} + M \frac{d\hat{I}}{dT} + RI + Hf(I)\omega = \Omega(MI + \hat{L}\hat{I}), \quad (2.77a)$$

$$L \frac{d\hat{I}}{dT} + M \frac{dI}{dT} + \hat{R}\hat{I} = 0, \quad (2.77b)$$

$$A \frac{d\Omega}{dT} = G - I(MI + \hat{L}\hat{I}) - K\Omega, \quad (2.77c)$$

$$B \frac{d\omega}{dT} = HI f(I) - D\omega, \quad (2.77d)$$

where  $2\pi L$  is the self-inductance of the coil,  $R$  is the total resistance of the dynamo circuit (including the coil and the armature of the motor),  $A$  is the moment of inertia of the disk and  $B$  that of the armature of the motor.

Equations (2.77a,b) respectively express Kirchoff's laws applied to the dynamo current,  $I$ , flowing in the main circuit and to the eddy current,  $\hat{I}$ , in the disk,  $\hat{R}$  being the azimuthal resistance of the disk (hereafter "disk resistance", the reciprocal of "disk conductance"). Equations (2.77c,d) express angular momentum considerations applied to the motion of the disk and to the motion of the armature of the motor respectively.

The equations can be studied by standard methods involving stability and bifurcation analysis and direct numerical integration. We note here in passing that if  $(I, \Omega, \omega, \hat{I})$  is a solution to (2.77b) then so is  $(-I, \Omega, -\omega, -\hat{I})$  when  $\varepsilon = 0$  and  $(-I, \Omega, \omega, -\hat{I})$  when  $\varepsilon = 1$ . However exact reversal is not a property of any of the solutions when  $0 < \varepsilon < 1$ . This does not imply that cases when  $\varepsilon \neq 1$  can have no geophysical or astrophysical significance. On the contrary, for the "external" contribution to the stationary ambient magnetic field within the motor could be due solely to the current in the coil of a second self-excited dynamo. It is readily shown that the combined system has the requisite symmetry properties.

#### 2.8.4. ENERGETICS AND EQUILIBRIUM SOLUTIONS.

Before introducing dimensionless variables and control parameters (see Section 2.8.5) and thereby abandoning a physically clear but mathematically cumbersome notation, it is instructive to discuss both the energetics of the system and equilibrium solutions on the basis of the dimensional equations (2.76) & (2.77). From these equations it is readily shown that the time rates-of-change of the total magnetic energy and the total mechanical energy of the system satisfy

$$\frac{d}{dT} \left[ \frac{1}{2} \left( LI^2 + 2MI\hat{I} + \hat{L}\hat{I}^2 \right) \right] = -RI^2 - \hat{R}\hat{I}^2 + \left\{ \Omega I \left( MI + \hat{L}\hat{I} \right) - \omega HI f(I) \right\}, \quad (2.78a)$$

$$\frac{d}{dT} \left[ \frac{1}{2} (A\Omega^2 + B\omega^2) \right] = G\Omega - K\Omega^2 - D\omega^2 - \left\{ \Omega I (MI + \widehat{L}\widehat{I}) - \omega H I f(I) \right\}. \quad (2.78b)$$

These equations have an obvious physical interpretation in terms of rates of working of mechanical and Lorentz forces and rates of dissipation by ohmic resistance to the flow of currents and by mechanical friction in the disk and motor. The nonlinear feedback and coupling terms in curly brackets represent the re-distribution of kinetic energy within the system brought about by Lorentz forces, and they cancel out when the equations are added together to give the equation for the rate of change of the total energy of the whole system.

Because we are considering the (important) special case when the applied couple,  $G$ , driving the system is steady, there are steady equilibrium solutions —albeit not always stable, as we shall see below in Section 2.8.6— for which the energy equations are given by equations (2.78) with their left hand sides equal to zero. The governing equations (2.76) & (2.77) are then autonomous and have steady equilibrium solutions satisfying

$$I \left[ \left( \frac{MG}{K} - R \right) - \left( \frac{M^2 I^2}{K} + \frac{H^2 f(I)^2}{D} \right) \right] = 0, \quad (2.79a)$$

$$\Omega = \frac{G - MI}{K}, \quad \omega = H I f(I), \quad \widehat{I} = 0. \quad (2.79b,c,d)$$

These equations always possess one “trivial” equilibrium solution

$$(I, \Omega, \omega, \widehat{I}) = (0, G/K, 0, 0), \quad (2.80)$$

and this is the only possible equilibrium solution when the dimensionless quantity  $GM/KR$  [see (2.82a) below] —which is analogous to the magnetic Reynolds number in MHD dynamos— is so small that the term in square brackets in (2.79a) is negative for all real values of  $I$ . Otherwise, when  $GM/KR$  is sufficiently large, there are two further equilibrium solutions with  $I \neq 0$ , obtained by substituting (2.79b) and (2.79c) into (2.79a). [*cf.* equations (2.84e) below].

## 2.8.5. DIMENSIONLESS EQUATIONS

The electro-mechanical characteristics of the system can be specified in terms of a set of dimensionless control parameters. Various combinations are possible, depending on the choice of scaling of the dependent and independent variables. Following Hide (1997a,1997b) (see also Hide & Moroz, 1999, and Hide, 2000) we take

$$\tilde{\alpha} = \frac{GLM}{AR^2}, \quad \tilde{\kappa} = \frac{KL}{AR}, \quad \xi = \frac{M}{L}, \quad (2.81a,b,c)$$

$$\chi = \frac{R\hat{L}}{\hat{R}L}, \quad \check{\nu} = \frac{\hat{L}}{M}, \quad (2.81d,e)$$

to specify the characteristics of the disk, and

$$\check{\beta} = \frac{H^2L}{R^2B}, \quad \check{\lambda} = \frac{DL}{RB}, \quad \check{\sigma} = S(G/M)^{1/2} \quad (2.81f,g,h)$$

to specify the characteristics of the series motor. Parameters (2.81a-h) as others in this section are noted with a  $\check{\cdot}$ . These variables will be used in the remaining of this chapter to describe the characteristics of the disk-motor setup. They should not be confused with MHD variables ( $\alpha, \beta, \kappa, \lambda, \mu, \nu, \rho, \sigma$ ) used elsewhere in the book.

It is convenient to make use of certain combinations of these basic control parameters, namely

$$\bar{\alpha} = \frac{\check{\alpha}}{\check{\kappa}} = \frac{GM}{KR}, \quad \bar{\beta} = \frac{\check{\beta}}{\check{\lambda}} = \frac{H^2}{RD}, \quad (2.82a,b)$$

$$\check{\mu} = \frac{(\xi/\check{\nu})}{(1 - \xi/\check{\nu})} = \frac{M^2}{L\hat{L} - M^2}. \quad (2.82c)$$

These control parameters are all essentially non-negative (including  $\check{\mu}$ , since  $L\hat{L} > M^2$ ) in systems of direct physical interest, but there may, of course, be mathematical interest in solutions of the governing equations in cases when some of the parameters are negative.

We introduce the dimensionless independent variable  $t$  and the dimensionless dependent variables  $(x(t), y(t), z(t), w(t))$  where

$$T = (L/R)t, \quad I = (G/M)^{1/2}x, \quad \Omega = (R/M)y, \quad (2.83a,b,c)$$

$$\omega = (LH/RB)(G/M)^{1/2}z, \quad \hat{I} = (G/M)^{1/2}w. \quad (2.83d,e)$$

Then using equations (2.81)–(2.83) in equations (2.76) and (2.77) gives<sup>4</sup>

$$\dot{x} + \xi\dot{w} = -x - \check{\beta}f(x)z + y(x + \check{\nu}w), \quad (2.84a)$$

$$\dot{w} + \dot{x}/\check{\nu} = -w/\chi, \quad (2.84b)$$

$$\dot{y} = \check{\alpha}(1 - x(x + \check{\nu}w)) - \check{\kappa}y, \quad (2.84c)$$

$$\dot{z} = xf(x) - \check{\lambda}z, \quad (2.84d)$$

where

$$f(x) = 1 - \varepsilon + \varepsilon\check{\sigma}x. \quad (2.84e)$$

This formulation is identical to that given in Hide & Moroz (1999) and Moroz & Hide (2000), with a slight redefinition of the control parameters.

<sup>4</sup> We use a dot to denote differentiation with respect to  $t$ .

The nontrivial equilibrium states are now given by

$$(y, z, w) = (\bar{\alpha}(1-x^2), x f(x)/\tilde{\lambda}, 0), \quad \bar{\alpha} - 1 - (\bar{\alpha}x^2 + \bar{\beta}f(x)^2) = 0, \quad (2.85a,b)$$

while the trivial equilibrium state becomes  $(x, y, z, w) = (0, \bar{\alpha}, 0, 0)$ .

Equations (2.84a-e) can be transformed into other sets of equations, some mathematically more convenient (see Hide & Moroz, 1999 and Moroz & Hide, 2000). One such reformulation not considered previously is obtainable by introducing  $X = x + \tilde{\nu}w$ , thereby eliminating the parameter  $\tilde{\nu}$ . If, in addition, one introduces the variable  $Y = x + \chi w$ , then one recovers the 4-mode dynamo model investigated by Hide & Moroz (1999) and Moroz & Hide (2000). The two new variables  $X$  and  $Y$  are identifiable as flux variables. The reader is referred to those papers for further details. All of the numerical integrations described in the later subsections of this section are based upon this alternative Moroz & Hide reformulation.

### 2.8.6. GENERIC SOLUTIONS

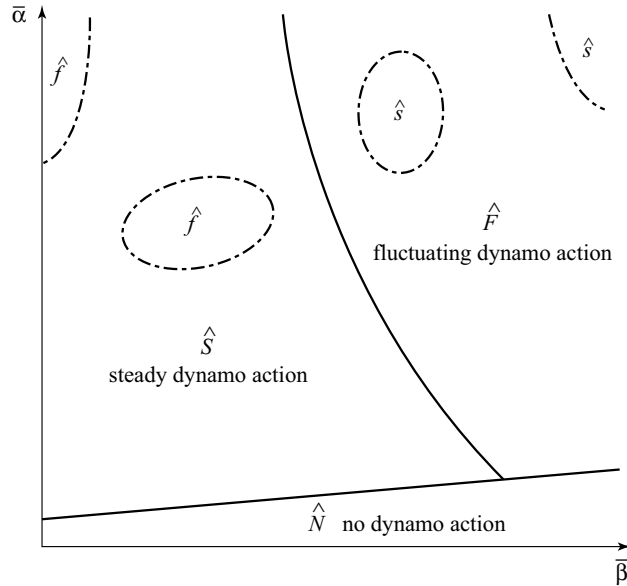
Nonlinearity means that the solutions in which we are mainly interested, namely those that persist after transients have died away, can be very sensitive to the initial conditions and/or parameter choices. A comprehensive investigation of the 4-mode dynamo equations is not feasible because of the large numbers of parameters involved. While the control parameters in any given case represent one point in an eight-dimensional parameter space, for many purposes a two-dimensional regime diagram with  $\bar{\beta}$  as abscissa and  $\bar{\alpha}$  as the ordinate was established at an early stage of the investigations reviewed here.

Figure 2.6 shows but one possibility amongst a wide variety of different regime diagrams that have been obtained in studies of the transformed version of equations (2.84a-e) (see Hide & Moroz, 1999, and Moroz & Hide, 2000).

The trivial equilibrium state  $(x, y, z, w) = (0, \bar{\alpha}, 0, 0)$  is the only stable equilibrium state within those regions  $\hat{N}$  (say) of parameter space for which  $\bar{\alpha} < \bar{\alpha}^*$ , where  $\bar{\alpha}^*$  is determined from whichever bifurcation curve forms that segment of the stability boundary (see, for example, Figure 1 of Hide & Moroz, 1999, or Figure 7 of Moroz & Hide, 2000). Persistent dynamo action cannot occur within  $N$ . It is throughout the rest of parameter space, in regions  $Y$ , say, where  $\bar{\alpha} > \bar{\alpha}^*$  that the trivial solution is unstable, that persistent dynamo action takes place.

Within these  $Y$  regions there are two general possibilities, namely *steady* dynamo action and *fluctuating* dynamo action.

The first occurs within regions labelled as  $\hat{S}$  and  $\hat{s}$  in Figure 2.6, or in the explicitly labelled 'STEADY' regions in Figures 1-3 of Hide & Moroz (1999) and in Figures 5-



**Figure 2.6** - Typical schematic regime diagram in the  $(\hat{\beta}, \bar{\alpha})$  plane (figure 1 of Hide (2000), reproduced by kind permission of the Royal Society). Within the region labelled  $\hat{N}$ , the parameter  $\bar{\alpha}$  (the effective “magnetic Reynolds number”) is too small for dynamo action to occur. At higher values of  $\bar{\alpha}$ , steady dynamo action occurs within the main region  $\hat{S}$  and sub-regions  $\hat{s}$ ; fluctuating dynamo action occurs within the main region  $\hat{F}$  and the sub-regions  $\hat{f}$ . The sub-regions disappear when the electrical properties of the disk are such that the azimuthal component of the current in the disk is negligible.

7 and Figure 9 of Moroz & Hide (2000). The initial conditions determine which of the two nontrivial equilibria obtain.

Fluctuating dynamo action occurs throughout the rest of  $Y$ , within regions labelled  $\hat{F}$  and  $\hat{f}$  in Figure 2.6 (or in the more explicitly labelled regime diagrams of Hide & Moroz, 1999, and Moroz & Hide, 2000), where the non-trivial equilibrium solutions lose their stability to large amplitude fluctuations of varying degrees of complexity, including multiple solutions and chaos (see below).

Self-excited dynamos, be they disk or MHD dynamos, satisfy essentially nonlinear equations, with generic solutions that are multiple and much more varied and interesting than just reflectionally- symmetric pairs [in MHD cases  $(\mathbf{u}, \mathbf{B})$  and  $(\mathbf{u}, -\mathbf{B})$ ], corresponding to an unaltered velocity field and a completely reversed magnetic field. We note here in passing (see below) that when  $0 < \varepsilon < 1$ , bias is automatically introduced into the fluctuating time series, regardless of its length. When  $\varepsilon = 0$  or  $\varepsilon = 1$ , the symmetry properties of the governing equations suggest that one

can define the length of time  $\tilde{T}$  taken for any bias in the time series to vanish.  $\tilde{T}$  is clearly infinite in the case of stable steady persistent solutions. On the other hand, for fluctuating persistent solutions  $\tilde{T}$  can of course be finite. Time series exhibiting these asymmetry/symmetry characteristics are presented in a later subsection.

## 2.8.7. SURVEY OF BEHAVIOUR

### VARIATIONS ON A THEME

Hide *et al.* (1996) extended the Bullard system by placing a capacitor in series with the coil and including mechanical friction in the disk and then demonstrated the mathematical equivalence of this system to one obtained by replacing the capacitor with a linear motor, with (unavoidable) mechanical friction in the motor equivalent to (unavoidable) leakage resistance in the capacitor. In this case the only non-zero parameters are  $\tilde{\alpha}$ ,  $\tilde{\beta}$ ,  $\tilde{\kappa}$  and  $\tilde{\lambda}$ .

We find it useful to employ the notation used in Section 2.8.5 above to summarise the results of extensions to the Hide *et al.* (1996) dynamo, including the one described by (2.84a-e).

- (a) a linear motor ( $\varepsilon = 0$ ) and no disk eddy currents ( $\chi = 0$ );

Case (a) is the original Hide *et al.* (1996) study in which the nonlinear dynamics was found to be controlled by the presence of a codimension-two Takens-Bogdanov double-zero bifurcation. The linear stability curves for steady and oscillatory dynamo action for both the trivial and the non-trivial states all emerge from one bifurcation point in  $(\tilde{\beta}, \tilde{\alpha})$ -space. Steady and fluctuating (periodic and chaotic) solutions are possible, with chaotic dynamics being confined to a small region of parameter space, near the (subcritical) Hopf stability boundary for the onset of oscillatory solutions associated with the nontrivial equilibria, provided  $\tilde{\lambda} > \tilde{\kappa}$ . When  $\tilde{\kappa} > \tilde{\lambda}$ , no chaotic solutions were observed.

- (b) a square motor ( $\varepsilon = 1$ ) and no disk eddy currents ( $\chi = 0$ );

Hide (1997b) considered the case of a square series motor so that  $\varepsilon = 1$  and found parameter space to be dominated by steady dynamo action. He termed this phenomenon 'nonlinear quenching'.

According to Hide (2000), nonlinear quenching is associated with the redistribution of kinetic energy within the system by Lorentz forces (see item (d) of Section 2.8.2 above), and if, as seems likely, the process is generic and therefore occurs in MHD dynamos, it could provide the basis of testable theory of geomagnetic polarity reversals, the most striking property of which is

the *absence* of reversals during very long intervals of time, the so-called “polarity superchrons”.

Mathematically, nonlinear quenching arises because, as noted by Moroz (2002), the Takens-Bogdanov double-zero bifurcation, responsible for the oscillatory solutions in the Hide *et al.* (1996) dynamo, now occurs at infinity.

- (c) a linear motor ( $\varepsilon = 0$ ) with azimuthal eddy currents ( $\chi \neq 0$ );

The extent to which this picture is changed when eddy currents are allowed to flow in the disk has been considered by treating systems for which the control parameters  $\chi$ ,  $\xi$  and  $\tilde{\nu}$  are no longer zero (Hide & Moroz, 1999). For a linear motor, the dynamics of the system is much richer than in the absence of eddy currents

$$\check{\rho} = \frac{\tilde{\nu}}{\chi(\tilde{\nu} - \xi)}, \quad \check{\mu} = \frac{\xi}{\tilde{\nu} - \xi}, \quad (2.86a,b)$$

then four scenarios are possible:

- (i) when  $\check{\rho} < \check{\lambda}(1 + \check{\mu})$ , only steady solutions are possible and nonlinear quenching occurs;
  - (ii) when  $\check{\lambda}(1 + \check{\mu}) < \check{\rho} < \check{\rho}_L$  (where  $\check{\rho}_L$  denotes the critical value of  $\check{\rho}$  for the existence of the Lorenz subcritical Hopf bifurcation for  $\check{\beta} = 0$ ), the scenario resembles that of Hide *et al.* (1996);
  - (iii) when  $\check{\rho} > \check{\rho}_L$ , parameter space is dominated by fluctuating solutions, either periodic or chaotic, with steady states occupying only a small region;
  - (iv) when  $\check{\lambda}(1 + \check{\mu}) > \check{\rho} > \check{\rho}_L$ , no double-zero bifurcation is possible and partial nonlinear quenching occurs. Oscillatory solutions are confined to small values of  $\check{\beta}$  and large values of  $\check{\alpha}$  and emanate from the subcritical Lorenz bifurcation point on the  $\check{\beta} = 0$  axis.
- (d) a square motor ( $\varepsilon = 1$ ) with azimuthal eddy currents ( $\chi \neq 0$ );  
In the cases when the motor is square (i.e.  $\varepsilon=1$ ) and eddy currents are allowed to flow in the disk, nonlinear quenching is still a key process, but it is again partial rather than complete in the sense defined in (c) above (Hide & Moroz, 1999).
- (e) a quadratic motor ( $0 < \varepsilon < 1$ ) with no azimuthal eddy currents ( $\chi = 0$ );  
Moroz (2002) extended the analyses of Hide *et al.* (1996) and Hide (1997a,b) to the case of a nonlinear series motor with  $0 < \varepsilon < 1$  in the absence of eddy currents. The double-zero bifurcations for the trivial and the nontrivial equilibria no longer coincide. There are multiple steady state bifurcation curves, as well as an additional Hopf bifurcation curve, which result in additional (non-degenerate) codimension-two Hopf-steady bifurcations. This yields a much

richer range of behaviour. The continuous range of chaotic solutions, a feature of case (a), now fragments and gives rise to a structure of interleaving chaotic and periodic behaviour of differing oscillatory patterns.

- (f) a quadratic motor ( $0 < \varepsilon < 1$ ) with azimuthal eddy currents ( $\chi \neq 0$ );  
 When  $0 < \varepsilon < 1$  and in the presence of eddy currents, the two double-zero bifurcations again become non-coincident and multiple steady and Hopf bifurcation curves generate a greater diversity of nonlinear behaviour than that found in case (e). Depending upon the parameter values, Moroz & Hide (2000) also found chaos occurring not far above the transitional curve for the onset of nontrivial dynamo action. Multiple solutions are possible and the nonlinear and linear stability thresholds are subject to hysteresis effects (see also the following subsection).

#### OTHER EXTENSIONS

Since the seminal work of Hide *et al.* (1996), other extensions to the basic dynamo systems have been investigated. Moroz *et al.* (1998a,b) investigated the behaviour of two coupled dynamo units with linear motors and in the absence of eddy currents. The first study confirmed the work of Hide (1995) on the structural instability of the Rikitake dynamo in the presence of even a small amount of friction, while the second study focused upon establishing general criteria for the existence of phase locked states. Moroz (2001) extended this study of synchronisation to a three dynamo configuration. The general problem of two coupled dynamos with nonlinear series motors was addressed in Moroz (2002), who also reviewed the research to date on the Hide family of dynamos to which the interested reader is also referred.

A start was made by Goldbrum *et al.* (2000) to analyse dynamo models, biased by immersion in a background magnetic field and/or by connecting a battery in series with the motor and coil (*cf.* the so-called ‘‘Biermann’’ battery of astrophysics), as given in Hide (1997a). The initial study was for the battery only, while Moroz (2001) investigated both the battery and magnetic field.

Finally, Moroz (2003, 2004) returned to the original Malkus–Robbins dynamo, extended to incorporate both a linear and a quadratic series motor, but in the absence of azimuthal eddy currents, to find different types of regime diagrams and different transition sequences between nonlinear states.

#### 2.8.8. SOME NUMERICAL INTEGRATIONS

In addition to the regime diagrams and behaviours described in Hide & Moroz (1999) and Moroz & Hide (2000), we present a selection of phase portraits, time

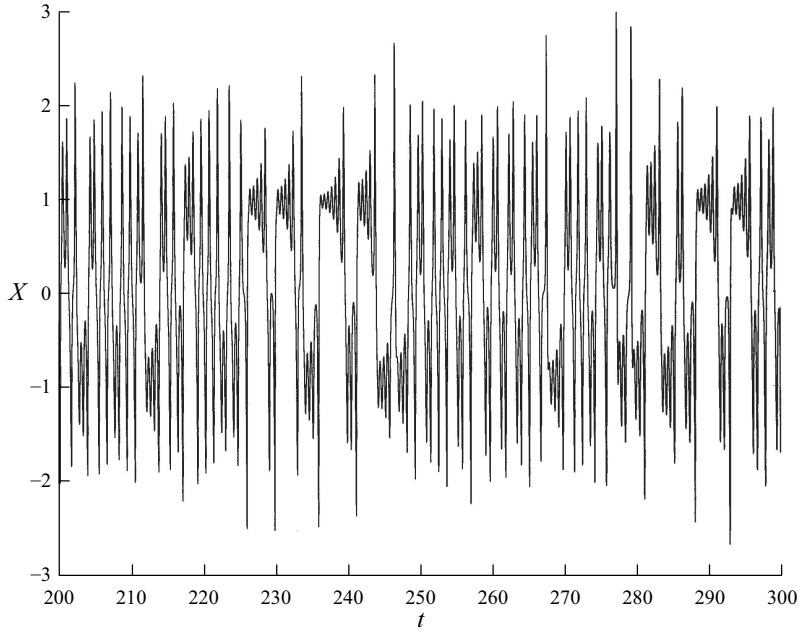


**Figure 2.7** - Time series of  $X$  for  $\varepsilon = 0$  and  $\tilde{\beta} = 5$ . The other parameters are given in the text.

series and bifurcation diagrams, which represent slices of parameter space for specific choices of the various parameters of the four-mode dynamo of Section 2.8.5 when re-written in the flux-formulation of Hide & Moroz (1999). In all of our integrations we chose  $\tilde{\alpha} = 100$ ,  $\tilde{\kappa} = 1$ ,  $\tilde{\lambda} = 1.2$ ,  $\tilde{\mu} = 0.5$  and  $\tilde{\rho} = 16$ , where  $\tilde{\mu}$  and  $\tilde{\rho}$  are defined in equation (2.86a,b). In so doing we shall demonstrate the existence of multiple solutions, as well as bias in the time series when  $0 < \varepsilon < 1$ .

#### $\varepsilon = 0$ AND $\varepsilon = 1$

The two cases reported in this subsection should be viewed in conjunction with Figures 1 & 2 of Hide & Moroz (1999).

When  $\varepsilon = 0$ , we have found that chaotic solutions persist for the range of  $\tilde{\beta}$  that we investigated, namely  $0 \leq \tilde{\beta} \leq 25$ . Figure 2.7 shows the time series of  $X$  and Figure 2.8 shows that corresponding phase portrait in the  $(X, w)$ -plane for  $\tilde{\beta} = 5$ .

When  $\varepsilon = 1$  and as described above, chaotic solutions are confined to much smaller regions of parameter space. Figure 2.9 shows a section of the  $X(t)$  time series and Figure 2.10 the phase portrait in  $(X, w)$ -space, for  $\tilde{\beta} = 0.4$  which is close to the transition from chaotic to steady dynamo action, when  $\tilde{\beta}$  is increased.

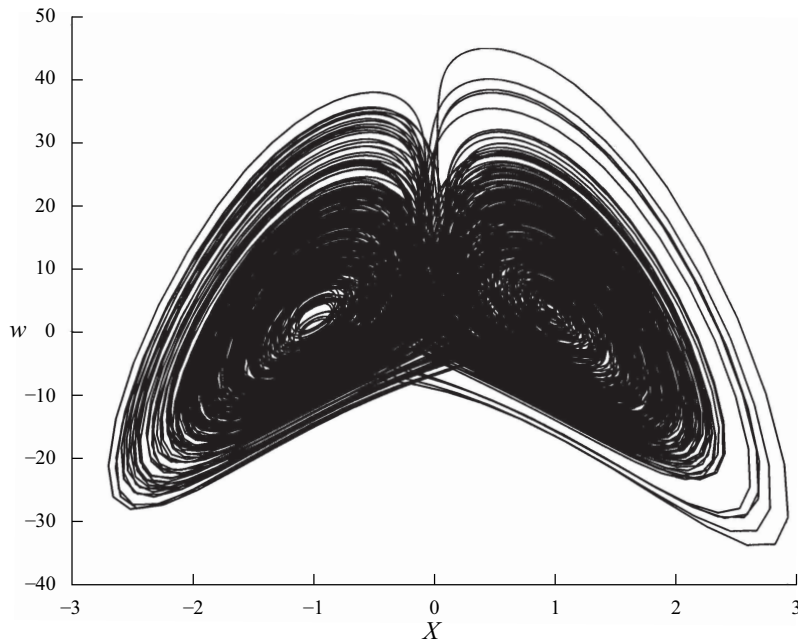


**Figure 2.8** - The phase portrait in the  $(X, w)$ -plane for the same parameter values as in Figure 2.7.

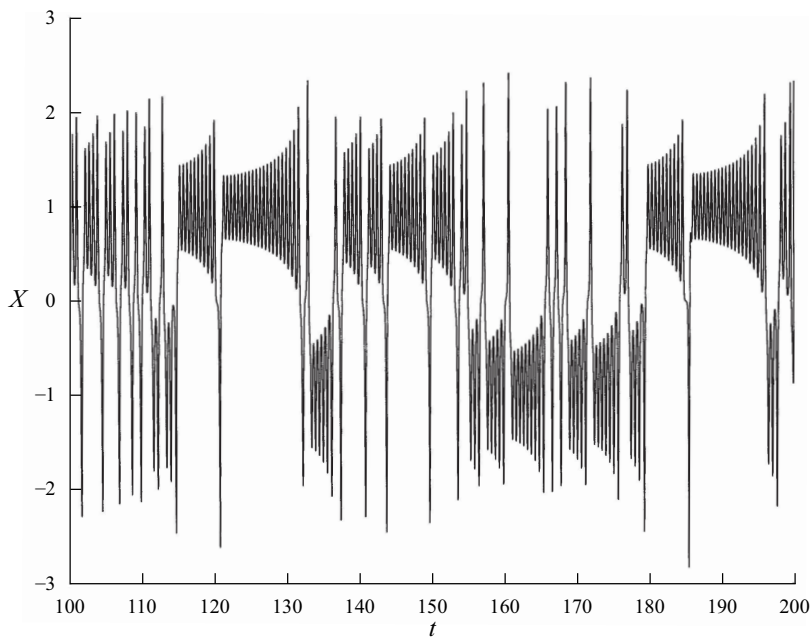


**Figure 2.9** - Times series of  $X$  for  $\varepsilon = 1$  and  $\check{\beta} = 0.4$ .

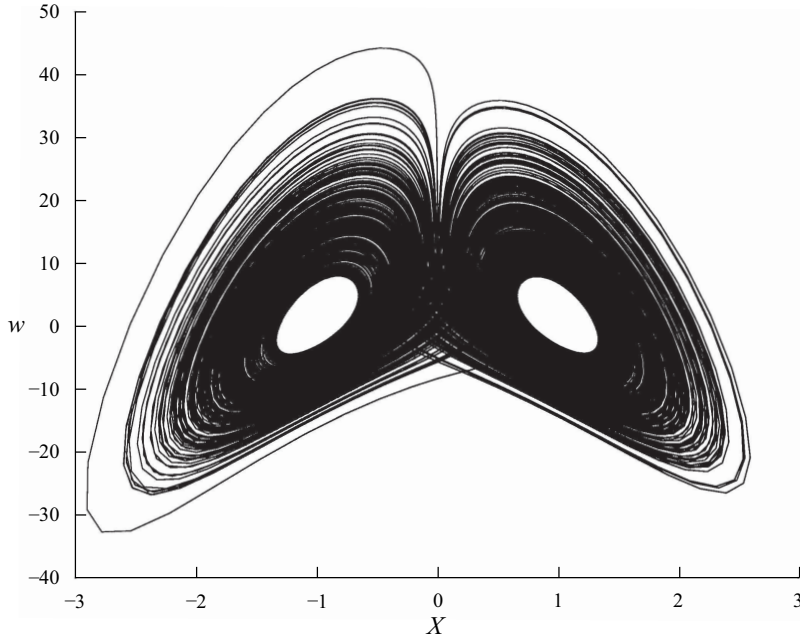


**Figure 2.10** - The phase portrait in the  $(X, w)$ -plane for the same parameter values as in Figure 2.9.

$$0 < \varepsilon < 1$$

We now amplify the results depicted in Figure 8 of Moroz & Hide (2000). Figure 2.11 shows the plot of local maximum values of  $X$  as a function of  $\check{\beta}$  for  $\varepsilon = 0.4$  as  $\check{\beta}$  is increased, while Figure 2.12 shows the corresponding plot when  $\check{\beta}$  is decreased. The procedure is as follows. The initial value of  $\check{\beta}$  is chosen and the maximum values of  $X$  are recorded after transients have decayed. Then  $\check{\beta}$  is increased/decreased and the final state is used as the initial condition for the next integration. This results in a bifurcation diagram, as a slice in parameter space, which affords a direct and simple way of identifying where different types of oscillatory behaviour may be found. Note the presence of windows of periodic solutions, separated by bands of chaotic solutions before the solution loses stability to a simple periodic solution when  $\check{\beta} \approx 10.3$ .

Figure 2.13 shows part of a time series for  $X$  when  $\check{\beta} = 6$  and  $\varepsilon = 0.4$  (cf. Figure 2.11(a)), while Figure 2.14 shows the corresponding phase portrait in the  $(X, w)$ -plane. Immediately apparent is the bias, introduced when  $\varepsilon$  differs from 0 or 1. The system spends more time oscillating (irregularly) around one of the (unstable) equilibrium states than it does around the other. A reversal in the time series occurs after a gradual build up in the maximum and minimum amplitudes.

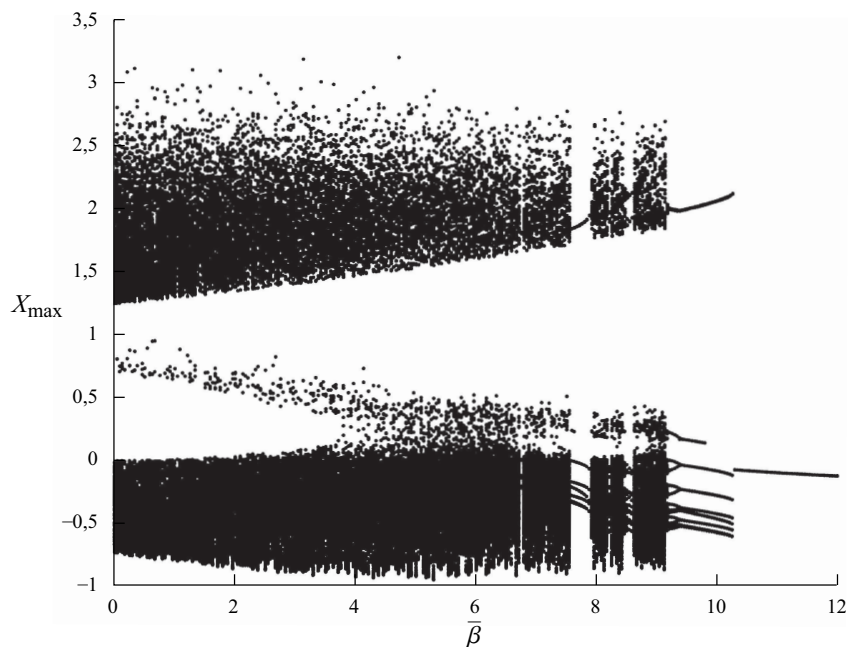


**Figure 2.11** - Plot of the local maximum value of  $X$  when  $\varepsilon = 0.4$ , as a function of  $\bar{\beta}$ , for  $\check{\beta}$  increasing.

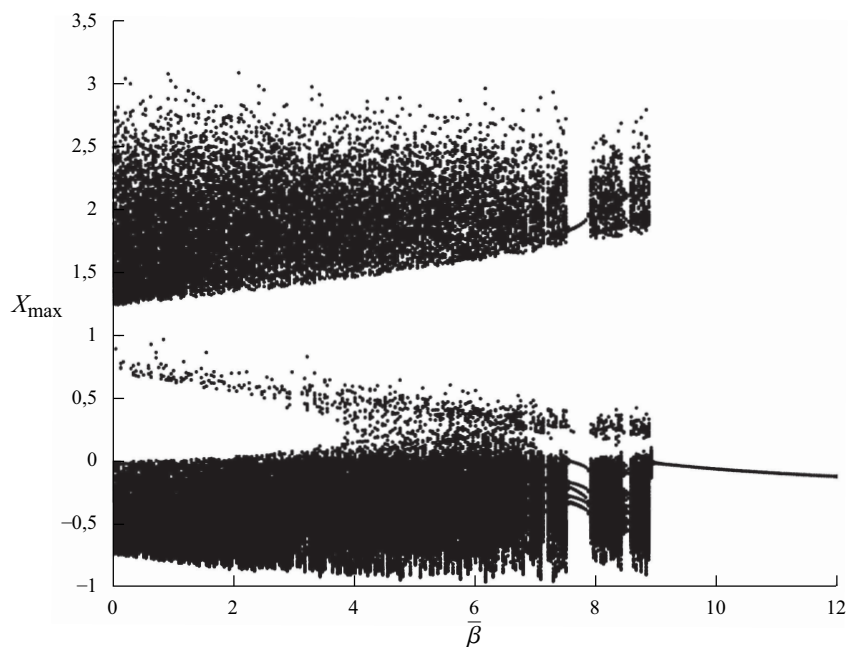


**Figure 2.12** - As in Figure 2.11, but for  $\check{\beta}$  decreasing.

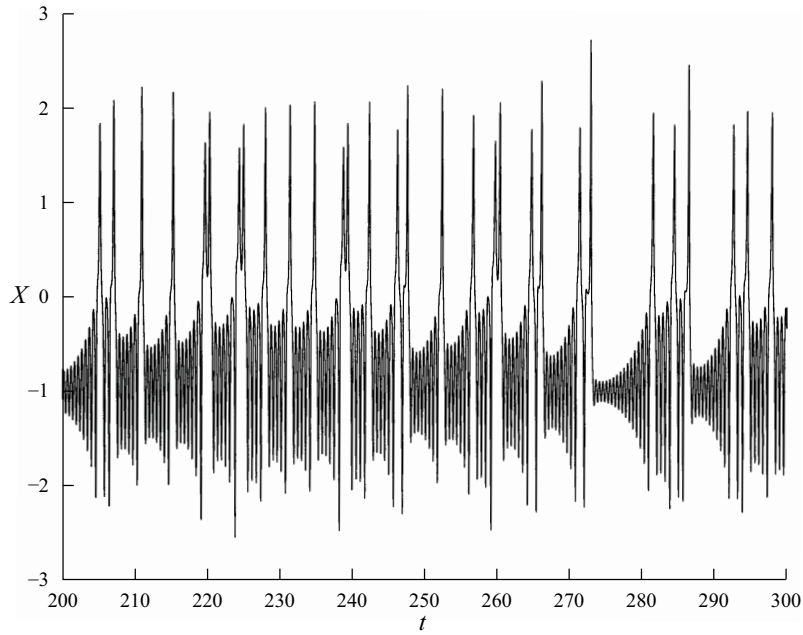


**Figure 2.13** - A section of the time series for  $X$  when  $\varepsilon = 0.4$  and  $\tilde{\beta} = 6$ .

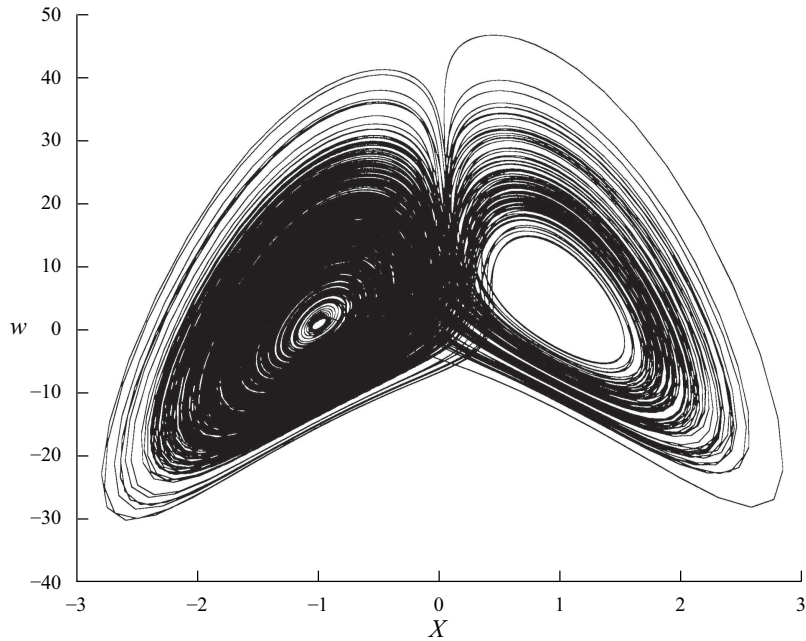


**Figure 2.14** - The phase portrait in the  $(X, w)$ -plane for the same parameter values as in Figure 2.13.

When  $\varepsilon = 0.535$  [*cf.* Figure 2.11(c)], chaotic solutions persist until  $\bar{\beta} \approx 4$ , when the system loses stability to a simple periodic limit cycle. This also persists until  $\bar{\beta} \approx 5.2$ , when steady dynamo action obtains. Figure 2.11(c) of Moroz & Hide (2000) suggests that the disappearance of oscillatory solutions could be caused by the presence of the branch  $H_3$  of periodic solutions.

In conclusion, this last section has presented a brief survey of some recent work which the authors and their collaborators have conducted on self-excited dynamos. As well as placing our own investigations into a historical context, we have made an effort to identify some key features of naturally-occurring MHD systems with their counterparts in the much lower-dimensional (and more tractable) Faraday-disk dynamos. Moreover care has been taken to ensure that the dynamo models studied exhibit structural stability, in contrast to the Bullard and Rikitake models.

In Section 2.8.6, we saw that features, generic to this class of dynamo are regions of parameter space in which no dynamo action, steady dynamo action and fluctuating dynamo action occur. The precise details as to where and which type of persistent behaviour dominates is, however, model and parameter dependent (see Section 2.8.7). Bifurcation transition sequences between different finite amplitude states are possible, in which chaotic and simple periodic behaviour interleave (see, for example, Figure 2.11). In addition, the nonlinear regime exhibits hysteresis with multiple solutions possible (see Section 2.8.8).

Other studies, referenced in Section 2.8.7, have introduced terms into the basic model, such as the effects of an external battery, which break the symmetry of the finite amplitude steady state solutions, as well as creating additional codimension-two bifurcations (Moroz, 2001b).

It is clear that this class of low order dynamo is capable of producing a rich range behaviours, depending upon both the parameters and the specific dynamo model chosen. What is required is some way of distinguishing between the whole gamut of possibilities. One such approach involves the identification of the underlying basis of unstable periodic orbits (UPOs), specific to a given model. Further investigations along these lines should prove rewarding.